

Numerical Methods for Chemotaxis and Related Models

Alexander Kurganov

Tulane University, Mathematics Department

`www.math.tulane.edu/~kurganov`

joint work with

Alina Chertock, North Carolina State University, USA

Yekaterina Epshteyn, University of Utah, USA

Klemens Fellner, University of Graz, Austria

Alexander Lorz, Université Pierre et Marie Curie, France

Mária Lukáčová-Medvid'ová, University of Mainz, Germany

Peter Markowich, University of Cambridge, UK

Patlak-Keller-Segel (PKS) Model

[Patlak; 1953], [Keller, Segel; 1970, 1971]

$$\begin{cases} \rho_t + \nabla \cdot (\chi \rho \nabla c) = \Delta \rho \\ \varepsilon c_t = \Delta c - c + \rho \end{cases} \quad \mathbf{x} = (x, y)^T \in \Omega, \quad t > 0$$

$\rho(x, y, t)$: cell density

$c(x, y, t)$: chemoattractant concentration

χ : chemotactic sensitivity constant

$\varepsilon = 1$: parabolic case

$\varepsilon = 0$: parabolic-elliptic case

- Solutions of this system may blow up in finite time
- This blow-up represents a mathematical description of a cell concentration phenomenon that occur in real biological systems

Naïve Finite-Difference Scheme

$$\begin{cases} \rho_t + (\chi\rho c_x)_x + (\chi\rho c_y)_y = \rho_{xx} + \rho_{yy} \\ c_t = c_{xx} + c_{yy} - c + \rho \end{cases}$$

$$\begin{cases} \frac{d\rho_{j,k}}{dt} = \frac{H^x_{j+\frac{1}{2},k} - H^x_{j-\frac{1}{2},k}}{\Delta x} - \frac{H^y_{j,k+\frac{1}{2}} - H^y_{j,k-\frac{1}{2}}}{\Delta y} + D_0^2\rho_{j,k} \\ \frac{dc_{j,k}}{dt} = D_0^2c_{j,k} - c_{j,k} + \rho_{j,k} \end{cases}$$

where

$$H^x_{j+\frac{1}{2},k} = \chi \frac{\rho_{j+1,k} + \rho_{j,k}}{2} \cdot \frac{c_{j+1,k} - c_{j,k}}{\Delta x}$$

$$H^y_{j,k+\frac{1}{2}} = \chi \frac{\rho_{j,k+1} + \rho_{j,k}}{2} \cdot \frac{c_{j,k+1} - c_{j,k}}{\Delta y}$$

$$D_0^2\rho_{j,k} = \frac{\rho_{j+1,k} - 2\rho_{j,k} + \rho_{j-1,k}}{(\Delta x)^2} + \frac{\rho_{j,k+1} - 2\rho_{j,k} + \rho_{j,k-1}}{(\Delta y)^2}$$

Example — Blowup at the Center of a Square Domain

$$\begin{cases} \rho_t + (\chi\rho c_x)_x + (\chi\rho c_y)_y = \rho_{xx} + \rho_{yy} \\ c_t = c_{xx} + c_{yy} - c + \rho \end{cases}$$

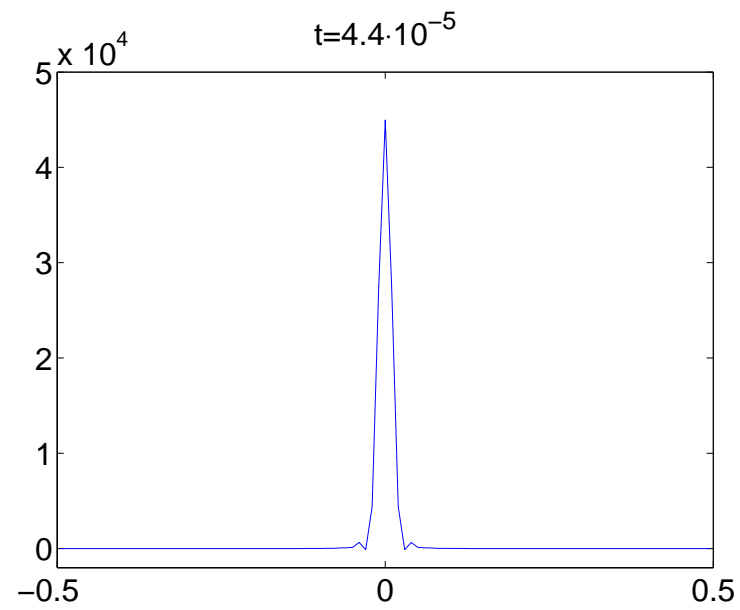
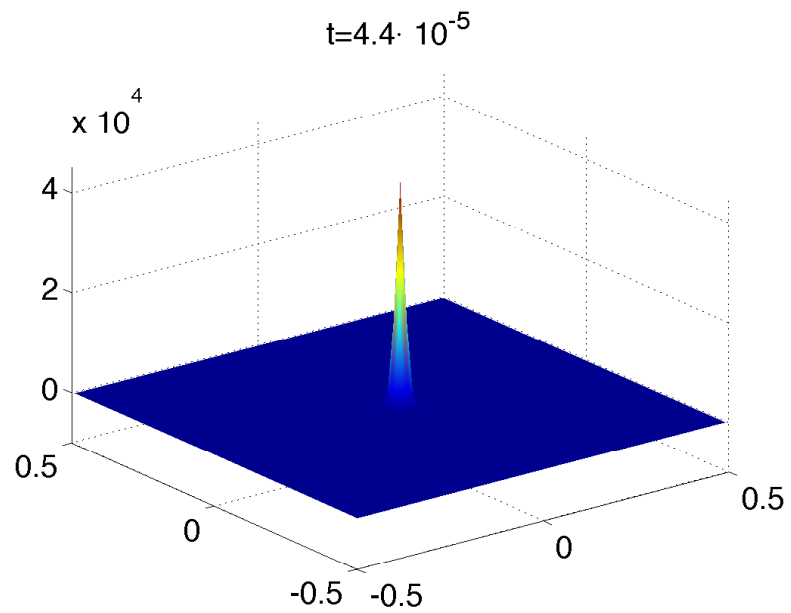
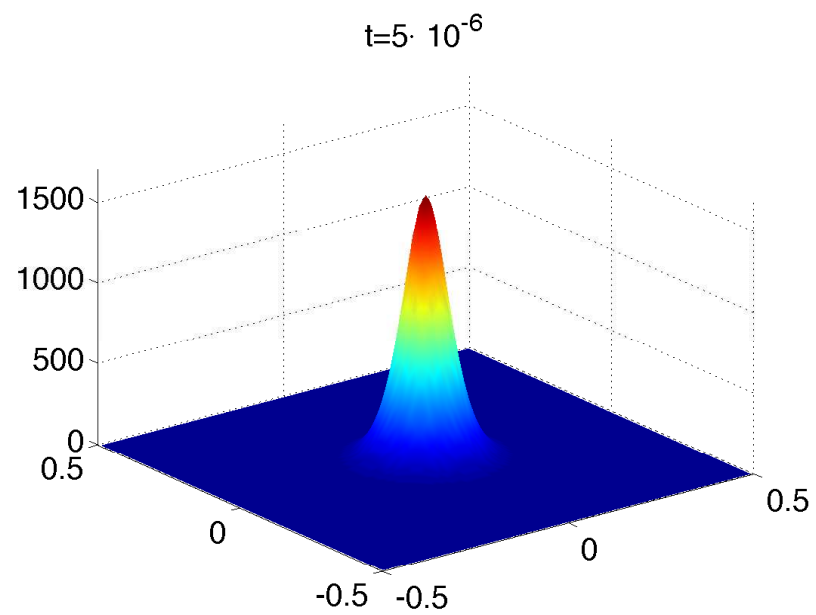
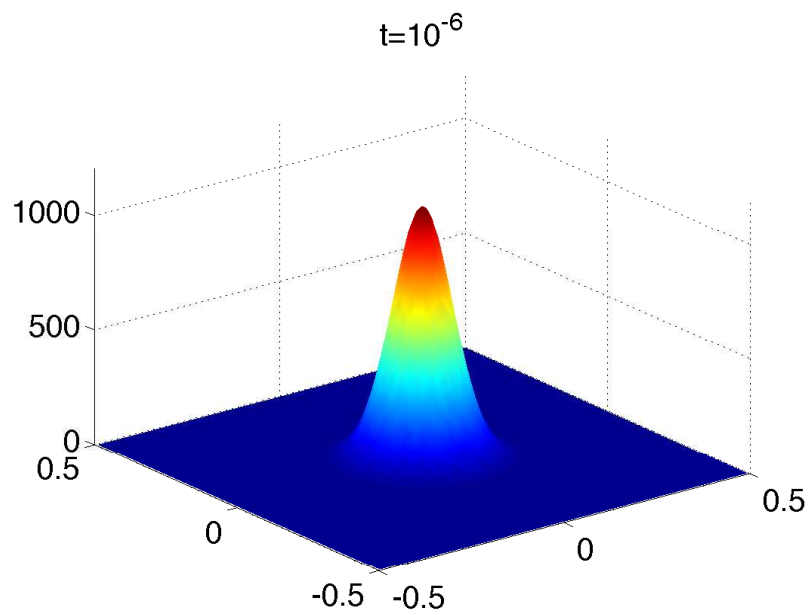
- Square domain $\Omega = [-\frac{1}{2}, \frac{1}{2}] \times [-\frac{1}{2}, \frac{1}{2}]$

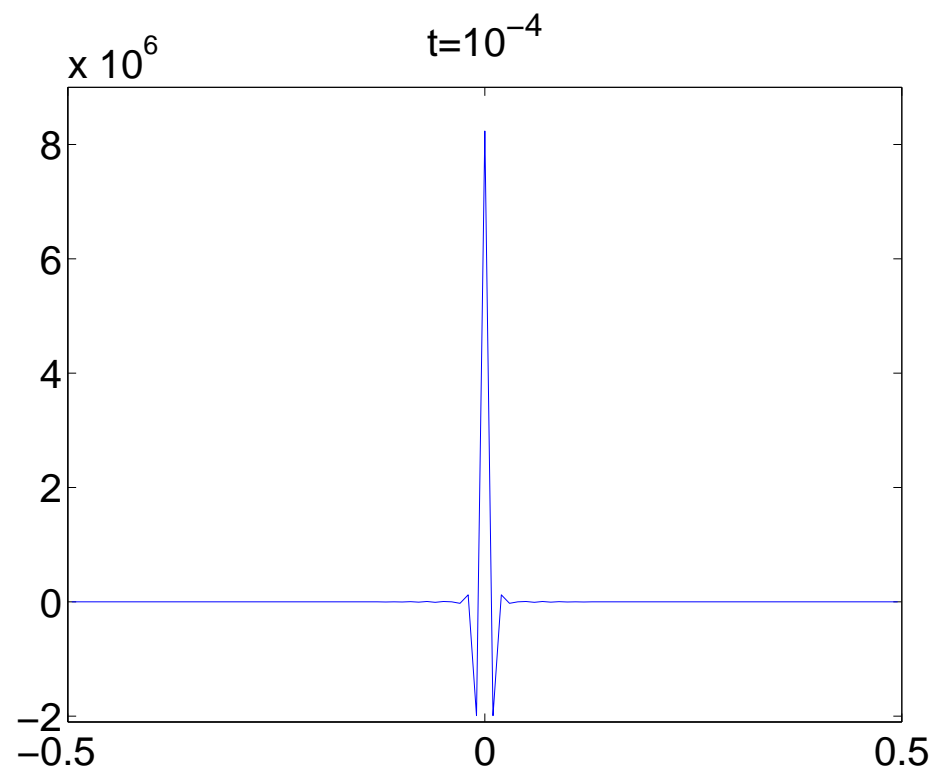
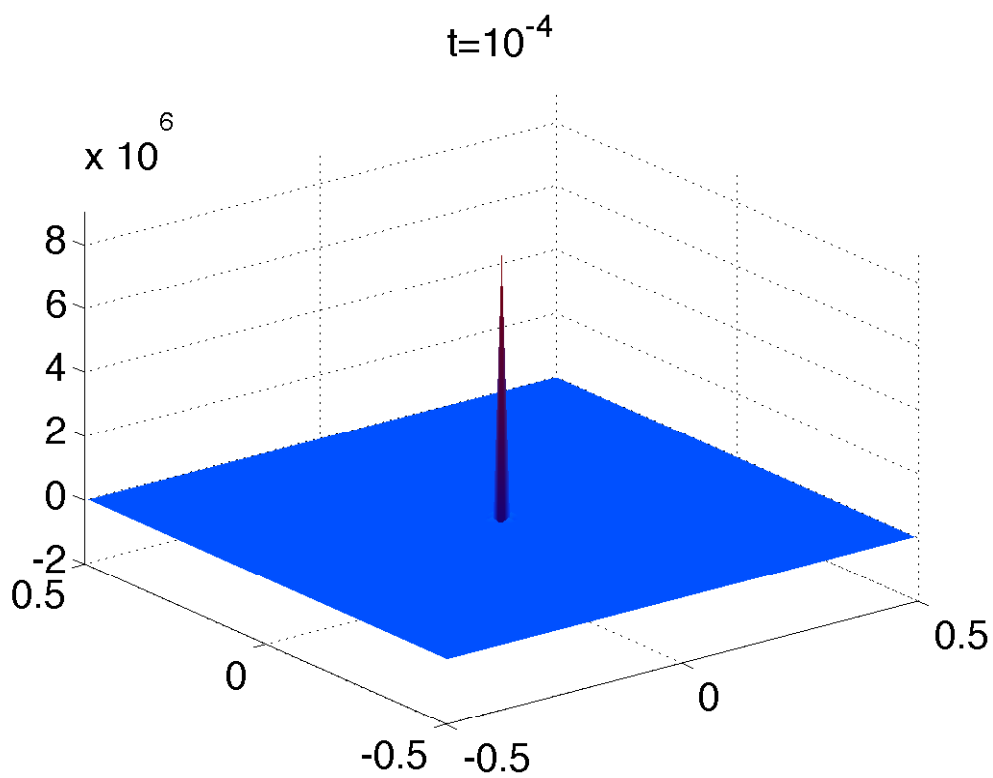
- Initial conditions:

$$\rho(x, y, 0) = 1000 e^{-100(x^2+y^2)}, \quad c(x, y, 0) = 500 e^{-50(x^2+y^2)}$$

- Neumann boundary conditions

According to [Harrero, Velázquez; 1997], both ρ - and c -components of the solution are expected to blow up at the origin in finite time.





Understanding the Nature of Instability

$$\begin{cases} \rho_t + (\chi\rho c_x)_x + (\chi\rho c_y)_y = \rho_{xx} + \rho_{yy} \\ c_t = c_{xx} + c_{yy} - c + \rho \end{cases}$$

Denote $u := c_x$ and $v := c_y$ and rewrite the PKS system

$$\begin{cases} \rho_t + (\chi\rho u)_x + (\chi\rho v)_y = \rho_{xx} + \rho_{yy} \\ u_t - \rho_x = u_{xx} + u_{yy} - u \\ v_t - \rho_y = v_{xx} + v_{yy} - v \end{cases}$$

This is a system of convection-diffusion-reaction equations:

$$\mathbf{U}_t + \mathbf{f}(\mathbf{U})_x + \mathbf{g}(\mathbf{U})_y = \Delta \mathbf{U} + \mathbf{R}(\mathbf{U})$$

$$\mathbf{U} := (\rho, u, v)^T, \quad \mathbf{f}(\mathbf{U}) := (\chi\rho u, -\rho, 0)^T, \quad \mathbf{g}(\mathbf{U}) := (\chi\rho v, 0, -\rho)^T,$$

$$\mathbf{R}(\mathbf{U}) := (0, -u, -v)^T.$$

$$\mathbf{U}_t + \mathbf{f}(\mathbf{U})_x + \mathbf{g}(\mathbf{U})_y = \Delta \mathbf{U} + \mathbf{R}(\mathbf{U})$$

$$\begin{pmatrix} \rho \\ u \\ v \end{pmatrix}_t + \begin{pmatrix} \chi \rho u \\ -\rho \\ 0 \end{pmatrix}_x + \begin{pmatrix} \chi \rho v \\ 0 \\ -\rho \end{pmatrix}_y = \begin{pmatrix} \Delta \rho \\ \Delta u \\ \Delta v \end{pmatrix} - \begin{pmatrix} 0 \\ u \\ v \end{pmatrix}$$

The **Jacobians** of \mathbf{f} and \mathbf{g} are:

$$\frac{\partial \mathbf{f}}{\partial \mathbf{U}} = \begin{pmatrix} \chi u & \chi \rho & 0 \\ -1 & 0 & 0 \\ 0 & 0 & 0 \end{pmatrix}, \quad \frac{\partial \mathbf{g}}{\partial \mathbf{U}} = \begin{pmatrix} \chi v & 0 & \chi \rho \\ 0 & 0 & 0 \\ -1 & 0 & 0 \end{pmatrix}$$

Their **eigenvalues** are:

$$\lambda_{1,2}^{\mathbf{f}} = \frac{\chi}{2} \left(u \pm \sqrt{u^2 - \frac{4\rho}{\chi}} \right), \quad \lambda_3^{\mathbf{f}} = 0$$

$$\lambda_{1,2}^{\mathbf{g}} = \frac{\chi}{2} \left(v \pm \sqrt{v^2 - \frac{4\rho}{\chi}} \right), \quad \lambda_3^{\mathbf{g}} = 0$$

The eigenvalues are:

$$\lambda_{1,2}^f = \frac{\chi}{2} \left(u \pm \sqrt{u^2 - \frac{4\rho}{\chi}} \right), \quad \lambda_3^f = 0$$
$$\lambda_{1,2}^g = \frac{\chi}{2} \left(v \pm \sqrt{v^2 - \frac{4\rho}{\chi}} \right), \quad \lambda_3^g = 0$$

The key observation: the “purely” convective system

$$\mathbf{U}_t + \mathbf{f}(\mathbf{U})_x + \mathbf{g}(\mathbf{U})_y = \mathbf{0}$$

is

- hyperbolic (real e-values) if both $\chi u^2 \geq 4\rho$ and $\chi v^2 \geq 4\rho$
- elliptic (complex e-values) if $\chi \min(u^2, v^2) < 4\rho$

Notice that the ellipticity condition is satisfied in generic cases, for example, when $u = c_x = 0$ and $\rho > 0$

The operator splitting approach may not be applicable!

Semi-Discrete Positivity Preserving Upwind Scheme

$$\begin{cases} \rho_t + (\chi\rho c_x)_x + (\chi\rho c_y)_y = \rho_{xx} + \rho_{yy} \\ c_t = c_{xx} + c_{yy} - c + \rho \end{cases}$$

Computational cells: $I_{j,k} := [x_{j-\frac{1}{2}}, x_{j+\frac{1}{2}}] \times [y_{k-\frac{1}{2}}, y_{k+\frac{1}{2}}]$

The cell averages of ρ , $\bar{\rho}_{j,k}(t) := \frac{1}{\Delta x \Delta y} \iint_{I_{j,k}} \rho(x, y, t) dx dy,$

and the point values of c , $c_{j,k} := c(x_j, y_k, t),$

are evolved in time by solving the system of ODEs:

$$\begin{cases} \frac{d\bar{\rho}_{j,k}}{dt} = \frac{H^x_{j+\frac{1}{2},k} - H^x_{j-\frac{1}{2},k}}{\Delta x} - \frac{H^y_{j,k+\frac{1}{2}} - H^y_{j,k-\frac{1}{2}}}{\Delta y} \\ \quad + \frac{\bar{\rho}_{j-1,k} - 2\bar{\rho}_{j,k} + \bar{\rho}_{j+1,k}}{(\Delta x)^2} + \frac{\bar{\rho}_{j,k-1} - 2\bar{\rho}_{j,k} + \bar{\rho}_{j,k+1}}{(\Delta y)^2} \\ \frac{dc_{j,k}}{dt} = \frac{c_{j-1,k} - 2c_{j,k} + c_{j+1,k}}{(\Delta x)^2} + \frac{c_{j,k-1} - 2c_{j,k} + c_{j,k+1}}{(\Delta y)^2} - c_{j,k} + \bar{\rho}_{j,k} \end{cases}$$

$$\{\bar{\rho}_{j,k}(t)\} \rightarrow \tilde{\rho}(\cdot, t) \rightarrow \{\rho_{j,k}^{\text{E,W,N,S}}(t)\} \rightarrow \left\{ \begin{array}{c} H_{j+\frac{1}{2},k}^x(t) \\ H_{j,k+\frac{1}{2}}^y(t) \end{array} \right\} \rightarrow \{\bar{\rho}_{j,k}(t+\Delta t)\}$$

(Discontinuous) piecewise-linear reconstruction:

$$\tilde{\rho}(x, y, t) := \bar{\rho}_{j,k} + (\rho_x)_{j,k}(x - x_j) + (\rho_y)_{j,k}(y - y_k), \quad (x, y) \in I_{j,k}$$

It is conservative, second-order accurate and non-oscillatory provided the slopes are computed by a nonlinear limiter

Example — the Generalized Minmod Limiter

$$\tilde{\rho}(x, y, t) := \bar{\rho}_{j,k} + (\rho_x)_{j,k}(x - x_j) + (\rho_y)_{j,k}(y - y_k), \quad (x, y) \in I_{j,k}$$

$$(\rho_x)_{j,k} = \text{minmod} \left(\theta \frac{\bar{\rho}_{j,k} - \bar{\rho}_{j-1,k}}{\Delta x}, \frac{\bar{\rho}_{j+1,k} - \bar{\rho}_{j-1,k}}{2\Delta x}, \theta \frac{\bar{\rho}_{j+1,k} - \bar{\rho}_{j,k}}{\Delta x} \right)$$

$$(\rho_y)_{j,k} = \text{minmod} \left(\theta \frac{\bar{\rho}_{j,k} - \bar{\rho}_{j,k-1}}{\Delta y}, \frac{\bar{\rho}_{j,k+1} - \bar{\rho}_{j,k-1}}{2\Delta y}, \theta \frac{\bar{\rho}_{j,k+1} - \bar{\rho}_{j,k}}{\Delta y} \right)$$

where $\theta \in [1, 2]$ and

$$\text{minmod}(z_1, z_2, \dots) := \begin{cases} \min_j \{z_j\}, & \text{if } z_j > 0 \quad \forall j \\ \max_j \{z_j\}, & \text{if } z_j < 0 \quad \forall j \\ 0, & \text{otherwise} \end{cases}$$

$$\{\bar{\rho}_{j,k}(t)\} \rightarrow \tilde{\rho}(\cdot, t) \rightarrow \left\{ \rho_{j,k}^{\text{E,W,N,S}}(t) \right\} \rightarrow \left\{ \begin{array}{c} H_{j+\frac{1}{2},k}^x(t) \\ H_{j,k+\frac{1}{2}}^y(t) \end{array} \right\} \rightarrow \{\bar{\rho}_{j,k}(t+\Delta t)\}$$

$\rho_{j,k}^{\text{E,W,N,S}}(t)$ are the point values of

$$\tilde{\rho}(x, y, t) = \bar{\rho}_{j,k} + (\rho_x)_{j,k}(x - x_j) + (\rho_y)_{j,k}(y - y_k), \quad (x, y) \in I_{j,k}$$

at $(x_{j+\frac{1}{2}}, y_k)$, $(x_{j-\frac{1}{2}}, y_k)$, $(x_j, y_{k+\frac{1}{2}})$ and $(x_j, y_{k-\frac{1}{2}})$, respectively:

$$\rho_{j,k}^{\text{E}} := \tilde{\rho}(x_{j+\frac{1}{2}} - 0, y_k) = \bar{\rho}_{j,k} + \frac{\Delta x}{2}(\rho_x)_{j,k}$$

$$\rho_{j,k}^{\text{W}} := \tilde{\rho}(x_{j-\frac{1}{2}} + 0, y_k) = \bar{\rho}_{j,k} - \frac{\Delta x}{2}(\rho_x)_{j,k}$$

$$\rho_{j,k}^{\text{N}} := \tilde{\rho}(x_j, y_{k+\frac{1}{2}} - 0) = \bar{\rho}_{j,k} + \frac{\Delta y}{2}(\rho_y)_{j,k}$$

$$\rho_{j,k}^{\text{S}} := \tilde{\rho}(x_j, y_{k-\frac{1}{2}} + 0) = \bar{\rho}_{j,k} - \frac{\Delta y}{2}(\rho_y)_{j,k}$$

$$\{\bar{\rho}_{j,k}(t)\} \rightarrow \tilde{\rho}(\cdot, t) \rightarrow \left\{ \rho_{j,k}^{E,W,N,S}(t) \right\} \rightarrow \left\{ \begin{array}{l} H_{j+\frac{1}{2},k}^x(t) \\ H_{j,k+\frac{1}{2}}^y(t) \end{array} \right\} \rightarrow \{\bar{\rho}_{j,k}(t+\Delta t)\}$$

$$H_{j+\frac{1}{2},k}^x = \chi \rho_{j+\frac{1}{2},k} u_{j+\frac{1}{2},k}, \quad H_{j,k+\frac{1}{2}}^y = \chi \rho_{j,k+\frac{1}{2}} v_{j,k+\frac{1}{2}}$$

$$u_{j+\frac{1}{2},k} = \frac{c_{j+1,k} - c_{j,k}}{\Delta x}, \quad v_{j,k+\frac{1}{2}} = \frac{c_{j,k+1} - c_{j,k}}{\Delta y}$$

$$\rho_{j+\frac{1}{2},k} = \begin{cases} \rho_{j,k}^E, & \text{if } u_{j+\frac{1}{2},k} > 0 \\ \rho_{j+1,k}^W, & \text{if } u_{j+\frac{1}{2},k} < 0 \end{cases}$$

$$\rho_{j,k+\frac{1}{2}} = \begin{cases} \rho_{j,k}^N, & \text{if } v_{j,k+\frac{1}{2}} > 0 \\ \rho_{j,k+1}^S, & \text{if } v_{j,k+\frac{1}{2}} < 0 \end{cases}$$

Positivity Preserving Property

Theorem: *The cell densities $\{\bar{\rho}_{j,k}(t)\}$, computed by the above second-order semi-discrete upwind scheme with a positivity preserving piecewise linear reconstruction for ρ , remain nonnegative provided the initial cell densities are nonnegative, the system of ODEs is discretized by a strong stability preserving (SSP) ODE solver, and the following CFL condition is satisfied:*

$$\Delta t \leq \min \left\{ \frac{\Delta x}{8a}, \frac{\Delta y}{8b}, \frac{(\Delta x)^2(\Delta y)^2}{4((\Delta x)^2 + (\Delta y)^2)} \right\}$$

where

$$a := \chi \max_{j,k} \left\{ \left| u_{j+\frac{1}{2},k} \right| \right\}, \quad b := \chi \max_{j,k} \left\{ \left| v_{j,k+\frac{1}{2}} \right| \right\}$$

Idea of Proof:

$$\begin{aligned}
 & \bar{\rho}_{j,k}(t + \Delta t) \\
 = & \left[\frac{1}{8} - \frac{\lambda\chi}{2} \left(|u_{j-\frac{1}{2},k}| - u_{j-\frac{1}{2},k} \right) \right] \rho_{j,k}^W + \left[\frac{1}{8} - \frac{\lambda\chi}{2} \left(|u_{j+\frac{1}{2},k}| + u_{j+\frac{1}{2},k} \right) \right] \rho_{j,k}^E \\
 & + \frac{\lambda\chi}{2} \left(|u_{j+\frac{1}{2},k}| - u_{j+\frac{1}{2},k} \right) \rho_{j+1,k}^W + \frac{\lambda\chi}{2} \left(|u_{j-\frac{1}{2},k}| + u_{j-\frac{1}{2},k} \right) \rho_{j-1,k}^E \\
 & + \left[\frac{1}{8} - \frac{\mu\chi}{2} \left(|v_{j,k-\frac{1}{2}}| - v_{j,k-\frac{1}{2}} \right) \right] \rho_{j,k}^S + \left[\frac{1}{8} - \frac{\mu\chi}{2} \left(|v_{j,k+\frac{1}{2}}| + v_{j,k+\frac{1}{2}} \right) \right] \rho_{j,k}^N \\
 & + \frac{\mu\chi}{2} \left(|v_{j,k+\frac{1}{2}}| - v_{j,k+\frac{1}{2}} \right) \rho_{j,k+1}^S + \frac{\mu\chi}{2} \left(|v_{j,k-\frac{1}{2}}| + v_{j,k-\frac{1}{2}} \right) \rho_{j,k-1}^N \\
 & + \bar{\rho}_{j,k} \left[\frac{1}{2} - \Delta t \left(\frac{2}{(\Delta x)^2} + \frac{2}{(\Delta y)^2} \right) \right] + \Delta t \left[\frac{\bar{\rho}_{j+1,k} + \bar{\rho}_{j-1,k}}{(\Delta x)^2} + \frac{\bar{\rho}_{j,k+1} + \bar{\rho}_{j,k-1}}{(\Delta y)^2} \right],
 \end{aligned}$$

where $\lambda \equiv \Delta t / \Delta x$ and $\mu \equiv \Delta t / \Delta y$.

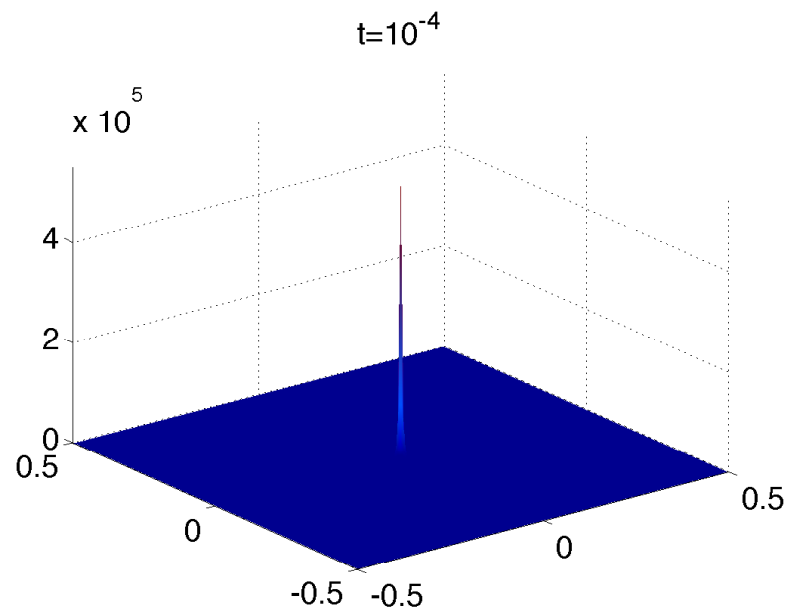
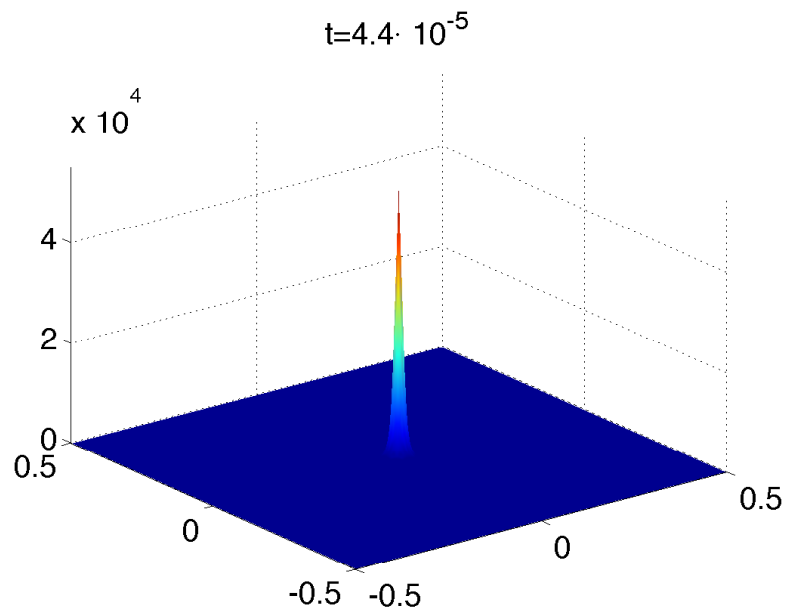
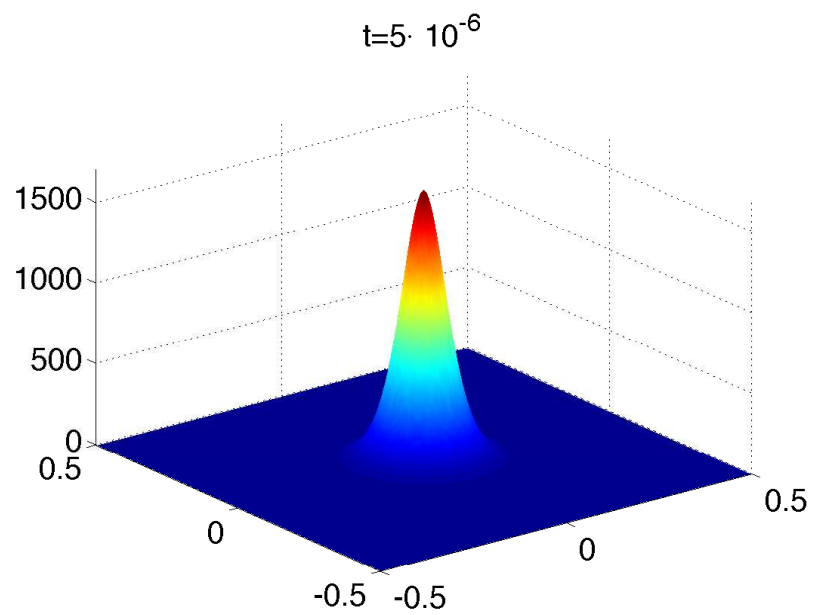
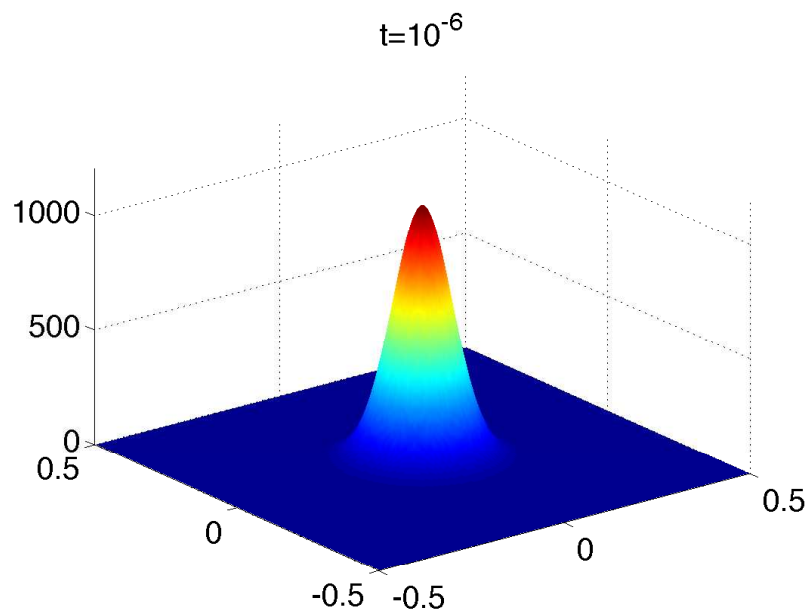
The new values $\{\bar{\rho}_{j,k}(t + \Delta t)\}$ are linear combinations of the nonnegative reconstructed point value $\{\rho_{j,k}^E, \rho_{j,k}^W, \rho_{j,k}^N, \rho_{j,k}^S\}$ and cell averages $\{\bar{\rho}_{j,k}\}$.

Example 1 — Blowup at the Center of a Square Domain

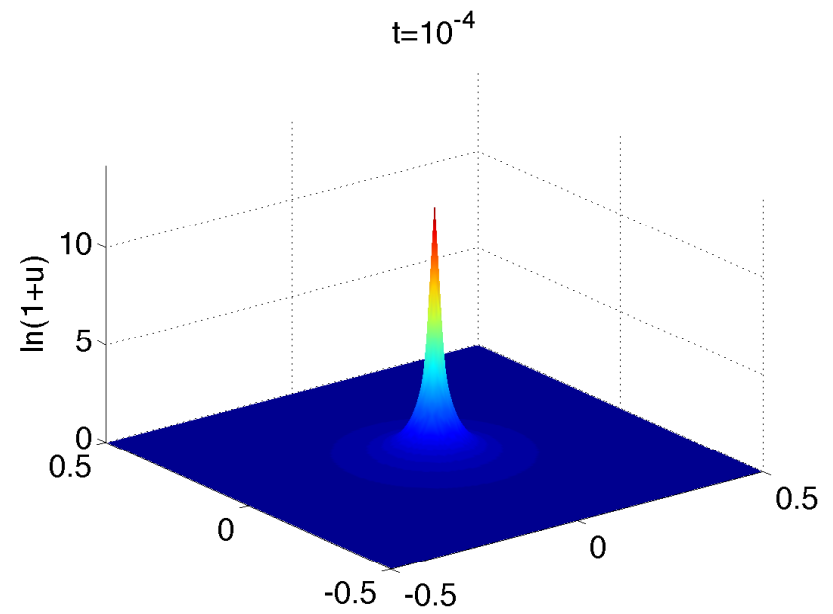
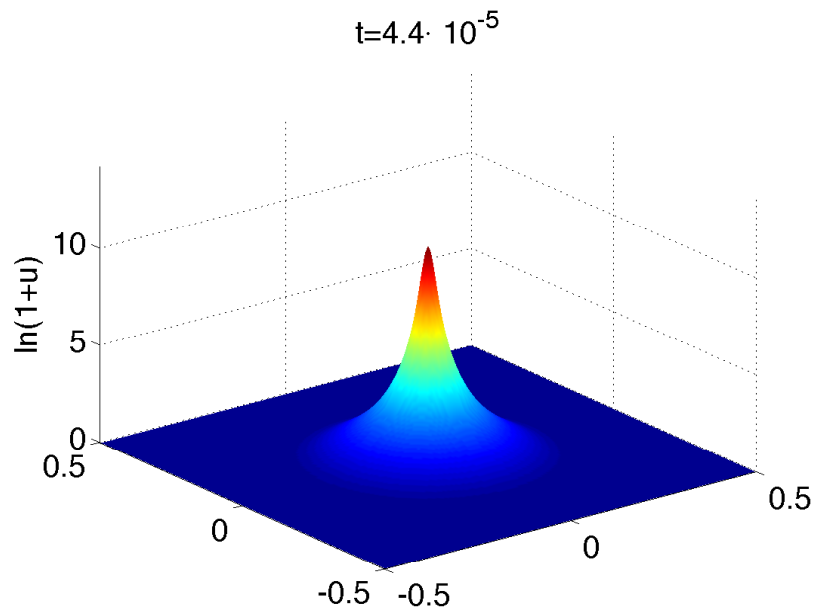
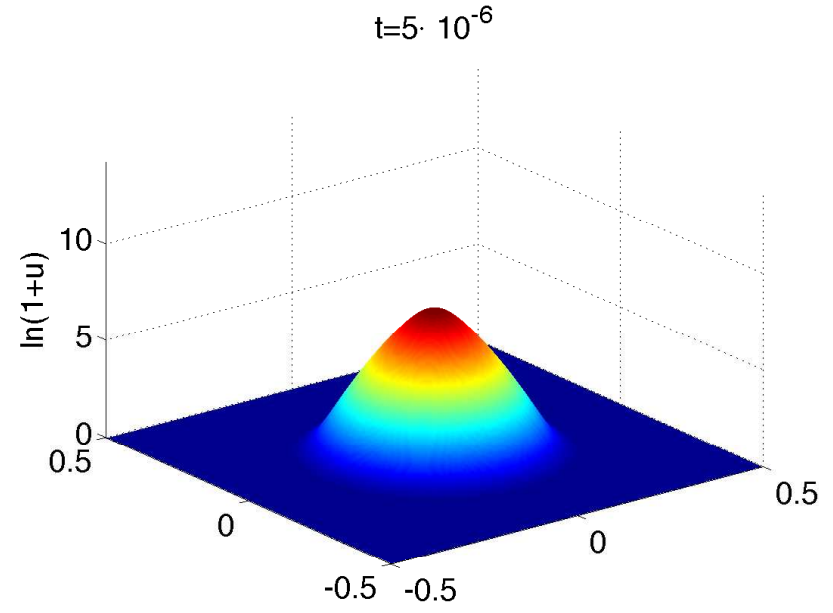
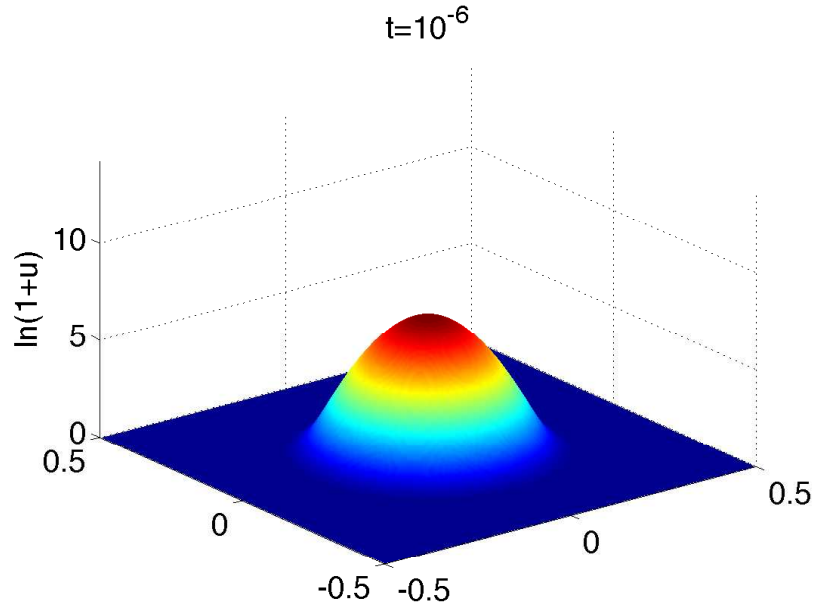
- Square domain $\Omega = [-\frac{1}{2}, \frac{1}{2}] \times [-\frac{1}{2}, \frac{1}{2}]$
- Radially symmetric bell-shaped initial data

$$\rho(x, y, 0) = 1000 e^{-100(x^2+y^2)}, \quad c(x, y, 0) = 500 e^{-50(x^2+y^2)}$$

- Neumann boundary conditions



Or, in the logarithmic vertical scale:



Example 2 — Blowup at the Center of a Square Domain

- Square domain $\Omega = [-\frac{1}{2}, \frac{1}{2}] \times [-\frac{1}{2}, \frac{1}{2}]$

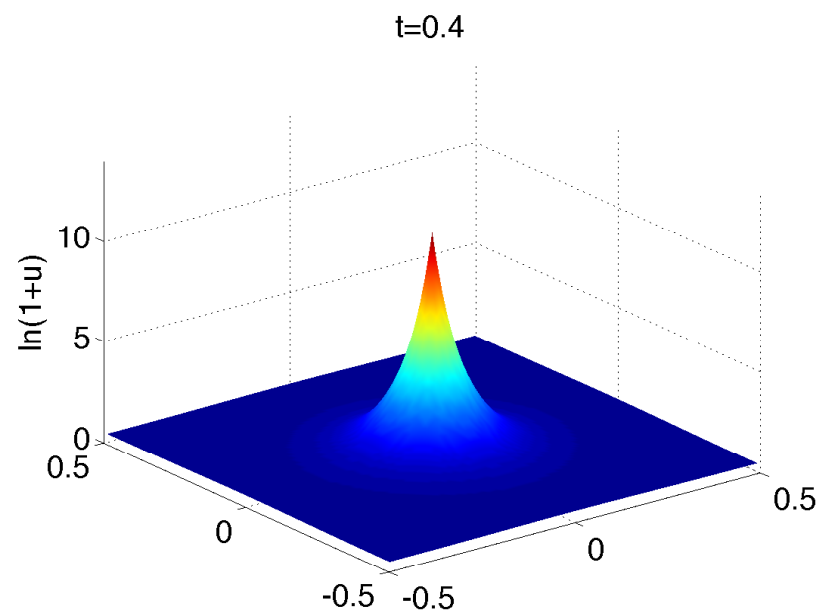
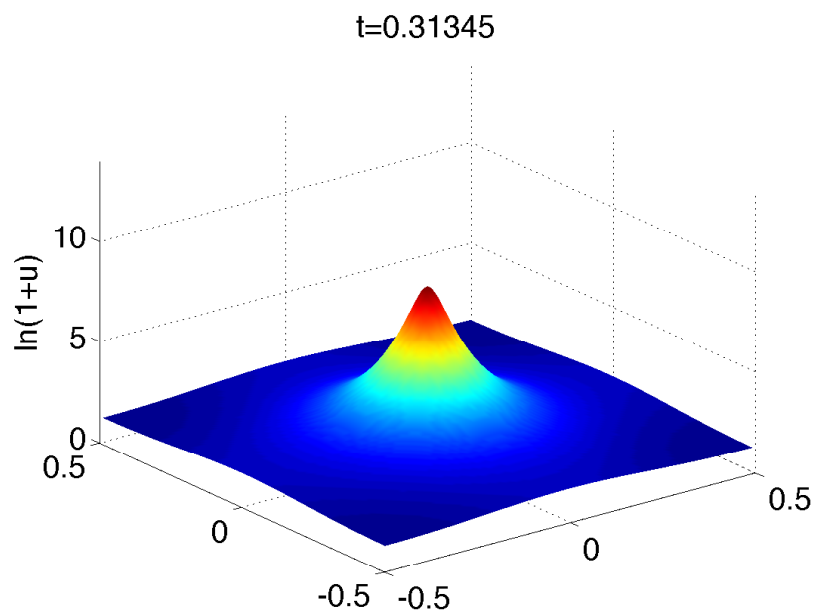
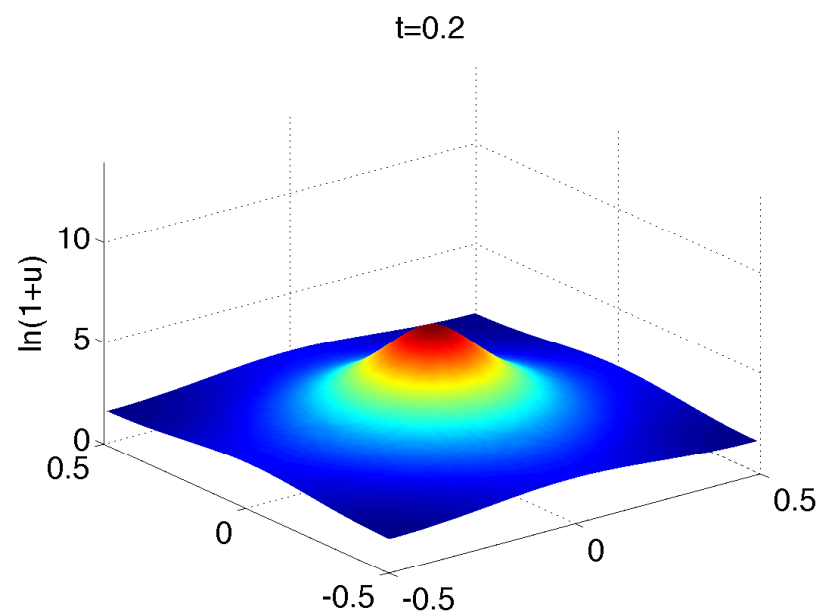
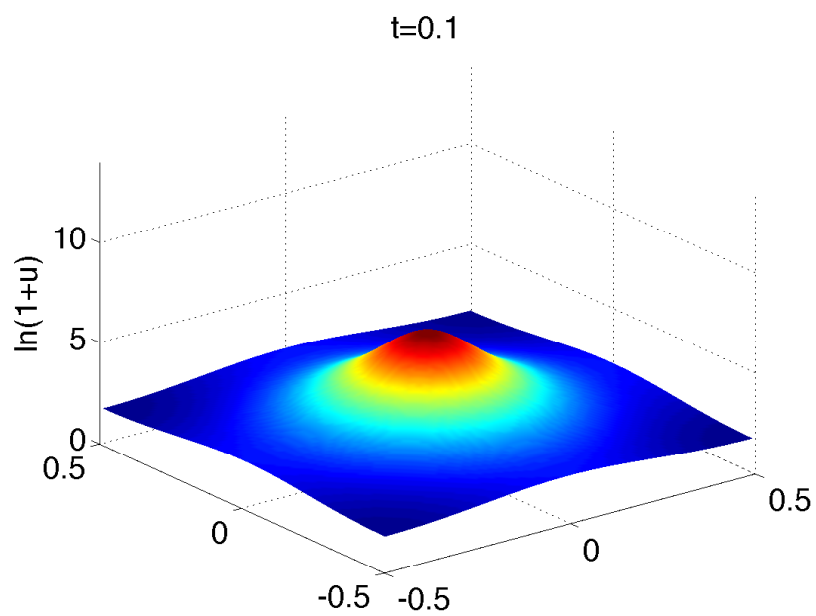
- Initial conditions:

$$\rho(x, y, 0) = 1000 e^{-100(x^2+y^2)}, \quad c(x, y, 0) \equiv 0$$

- Neumann boundary conditions

Properties:

- both ρ - and c -components of the solution are expected to blow up at the origin in finite time;
- the blowup is expected to occur later than in Example 1;
- the diffusion initially dominates the concentration mechanism and hence, the cells spread out and the cell density maximum decreases at small times.



Example 3 — Blowup at the Corner of a Square Domain

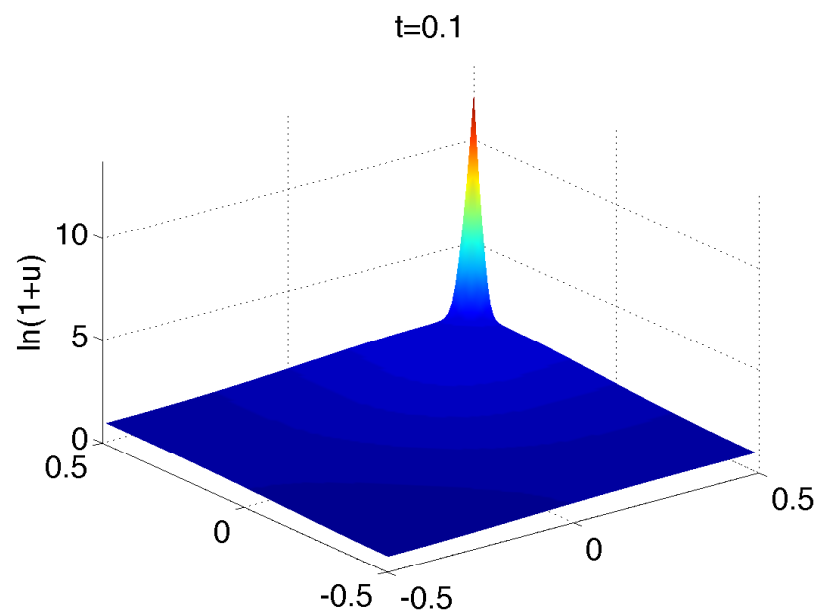
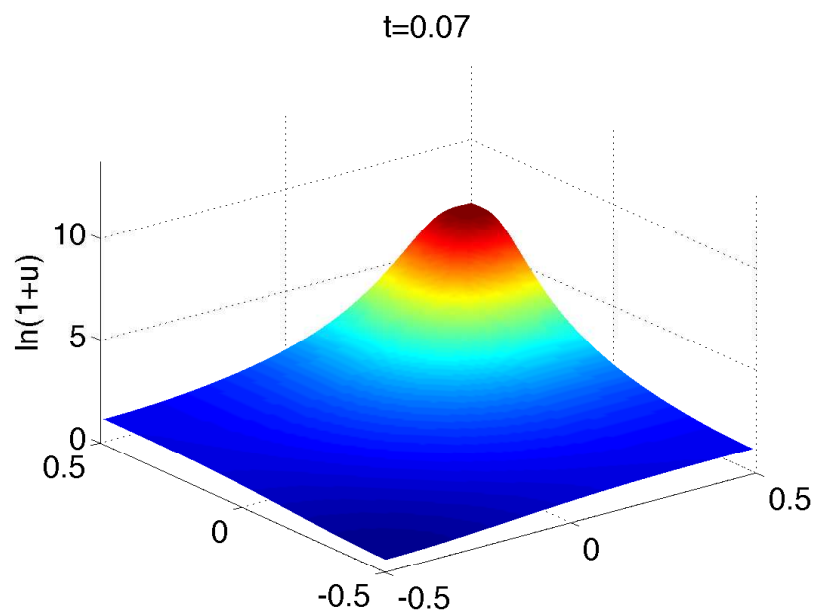
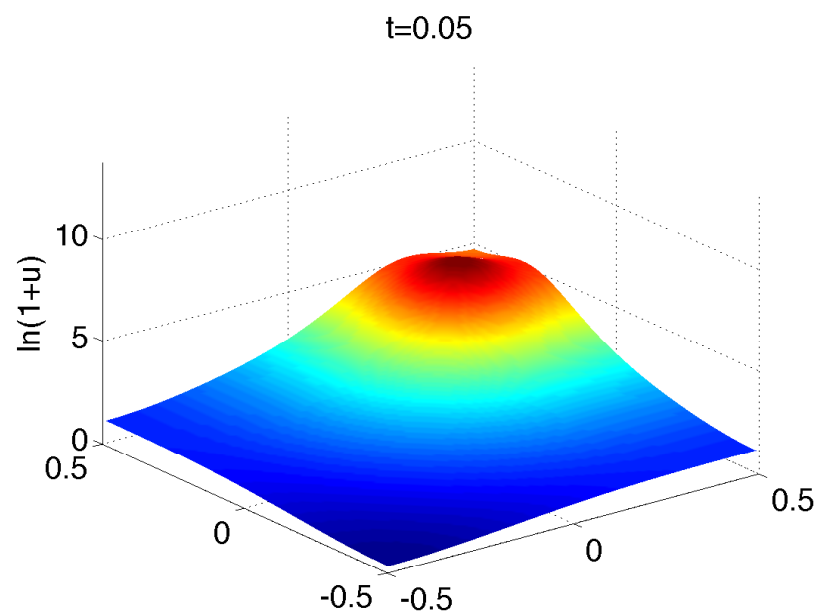
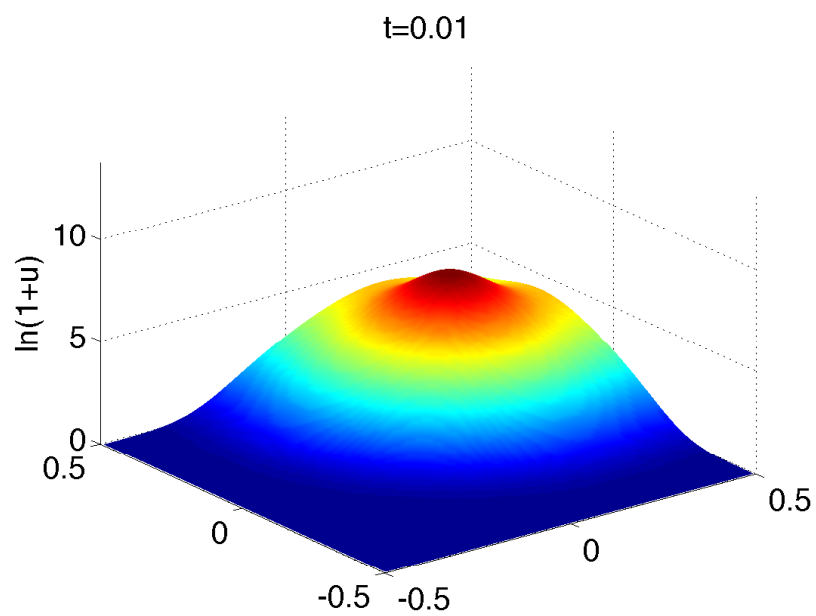
- Square domain $\Omega = [-\frac{1}{2}, \frac{1}{2}] \times [-\frac{1}{2}, \frac{1}{2}]$

- Initial conditions:

$$\rho(x, y, 0) = 1000 e^{-100((x-0.25)^2 + (y-0.25)^2)}, \quad c(x, y, 0) \equiv 0$$

- Neumann boundary conditions

The solution is expected to blow up at the corner $(\frac{1}{2}, \frac{1}{2})$



Two-Species Chemotaxis Models

$$\begin{cases} (\rho_1)_t + \chi_1 \nabla \cdot (\rho_1 \nabla c) = \mu_1 \Delta \rho_1 \\ (\rho_2)_t + \chi_2 \nabla \cdot (\rho_2 \nabla c) = \mu_2 \Delta \rho_2 \\ \Delta c + \gamma_1 \rho_1 + \gamma_2 \rho_2 - \zeta c = 0 \end{cases} \quad \mathbf{x} \in \Omega \subset \mathbb{R}^d, \quad t > 0$$

Assume that

$$\chi_1 < \chi_2$$

According to

[Wolansky; 2002]

[Espejo, Stevens, Velázquez; 2010]

[Conca, Espejo, Vilches; 2011]

[Espejo, Stevens, Suzuki; 2012]

[Espejo, Vilches, Conca; to appear]

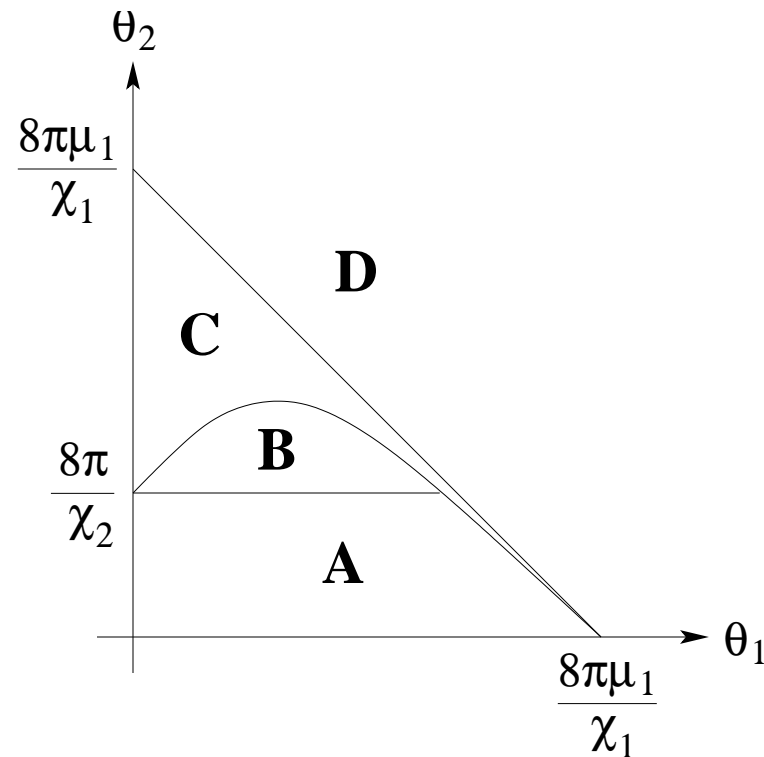
the solution may either be globally regular or both ρ_1 and ρ_2 would blow up within a finite time

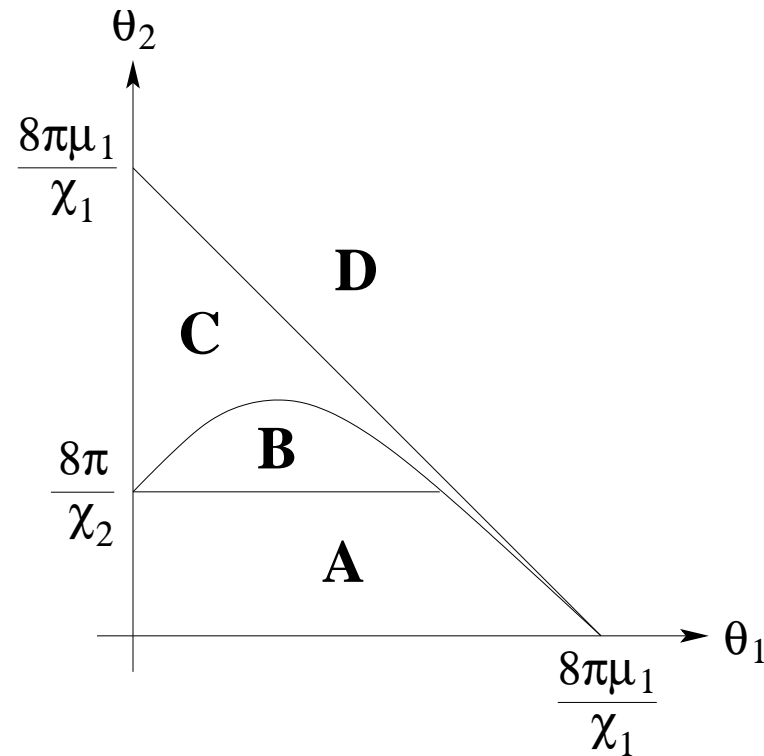
More precisely, for the IVP for the system

$$\begin{cases} (\rho_1)_t + \chi_1 \nabla \cdot (\rho_1 \nabla c) = \mu_1 \Delta \rho_1 \\ (\rho_2)_t + \chi_2 \nabla \cdot (\rho_2 \nabla c) = \Delta \rho_2 \\ \Delta c + \rho_1 + \rho_2 - c = 0 \end{cases} \quad \mathbf{x} \in \Omega \equiv \mathbb{R}^d, \quad t > 0$$

the behavior of the solution depends on the total masses

$$\theta_1 := \int_{\Omega} \rho_1(\mathbf{x}, t) d\mathbf{x} = \int_{\Omega} \rho_1^0(\mathbf{x}) d\mathbf{x}, \quad \theta_2 := \int_{\Omega} \rho_2(\mathbf{x}, t) d\mathbf{x} = \int_{\Omega} \rho_2^0(\mathbf{x}) d\mathbf{x}$$





- There is a **global classical solution** in Region **A**
- In Region **C**, ρ_2 **blows up faster** than ρ_1
- In Region **D**, ρ_1 and ρ_2 **blow up at the same rate**

The question on the solution behavior in Region **B** remains **open**

Example 1 — Global Existence in Region A

- Square domain $\Omega = [-\frac{3}{2}, \frac{3}{2}] \times [-\frac{3}{2}, \frac{3}{2}]$

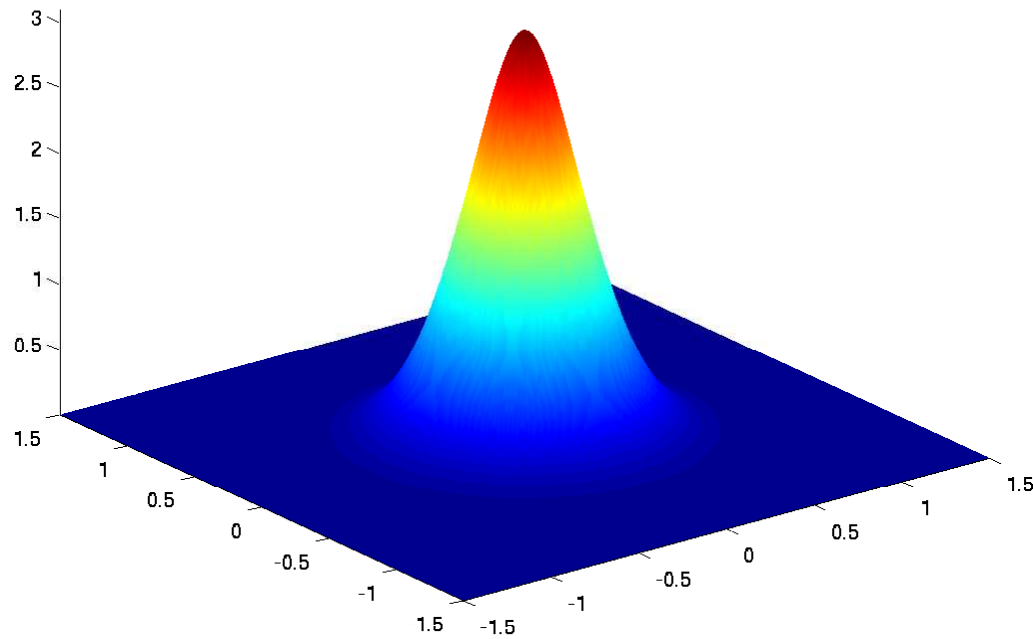
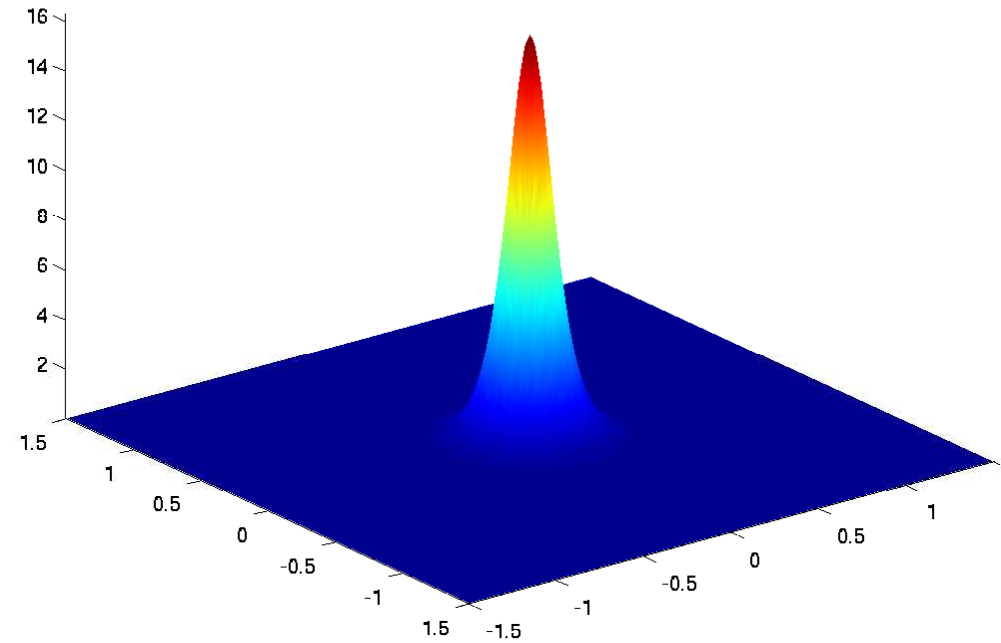
- Initial conditions:

$$\rho_1(x, y, 0) \equiv \rho_2(x, y, 0) = 50 e^{-100(x^2+y^2)}$$

- Parameters:

$$\chi_1 = 1, \quad \chi_2 = 10, \quad \mu_1 = 1$$

- Neumann boundary conditions

ρ_1  ρ_2 

The magnitude of both ρ_1 and ρ_2 decays and the solution remains smooth and bounded

Example 2 — ρ_2 Blows Up Faster than ρ_1 in Region C

- Square domain $\Omega = [-\frac{3}{2}, \frac{3}{2}] \times [-\frac{3}{2}, \frac{3}{2}]$

- Initial conditions:

$$\rho_1(x, y, 0) = 10 e^{-100(x^2+y^2)}, \quad \rho_2(x, y, 0) = 90 e^{-100(x^2+y^2)}$$

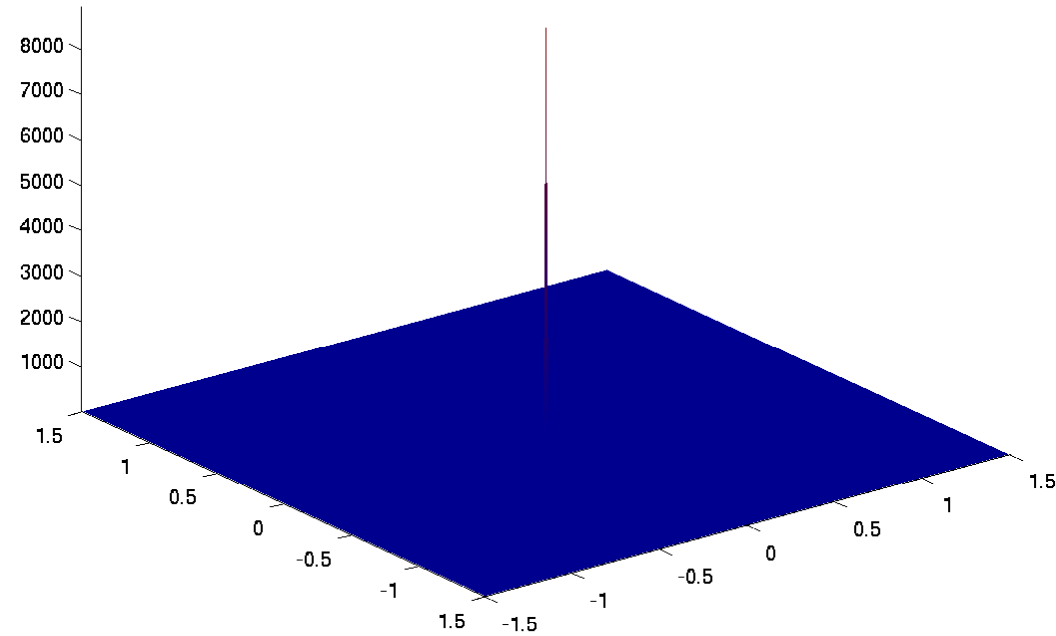
- Parameters:

$$\chi_1 = 6, \quad \chi_2 = 100, \quad \mu_1 = 1$$

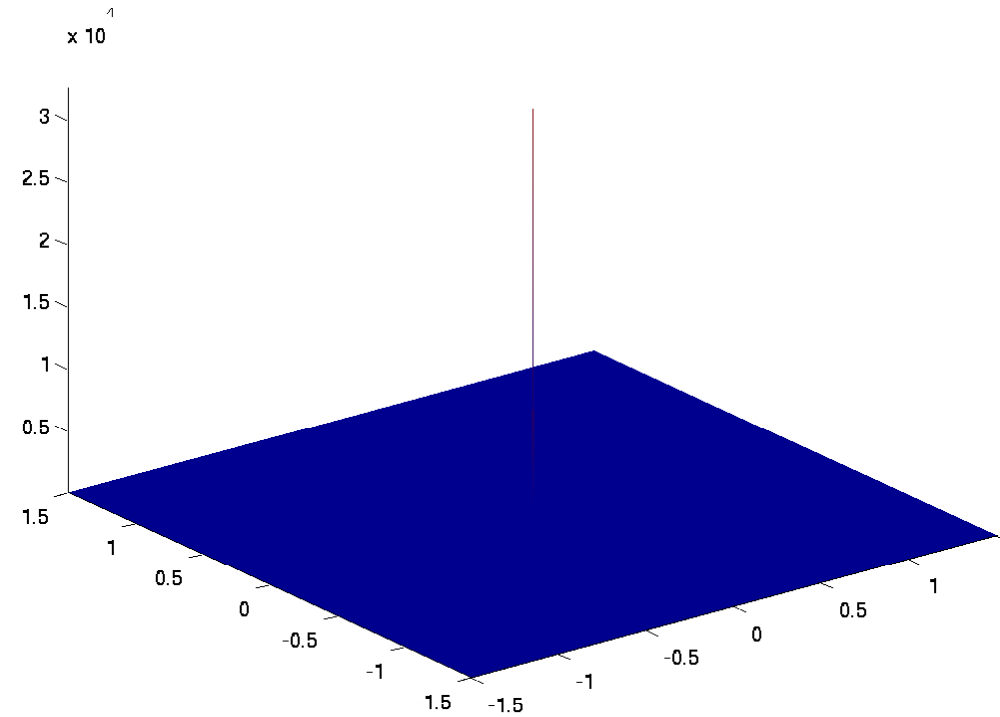
- Neumann boundary conditions

200 × 200 vs. 400 × 400

ρ_2



ρ_2



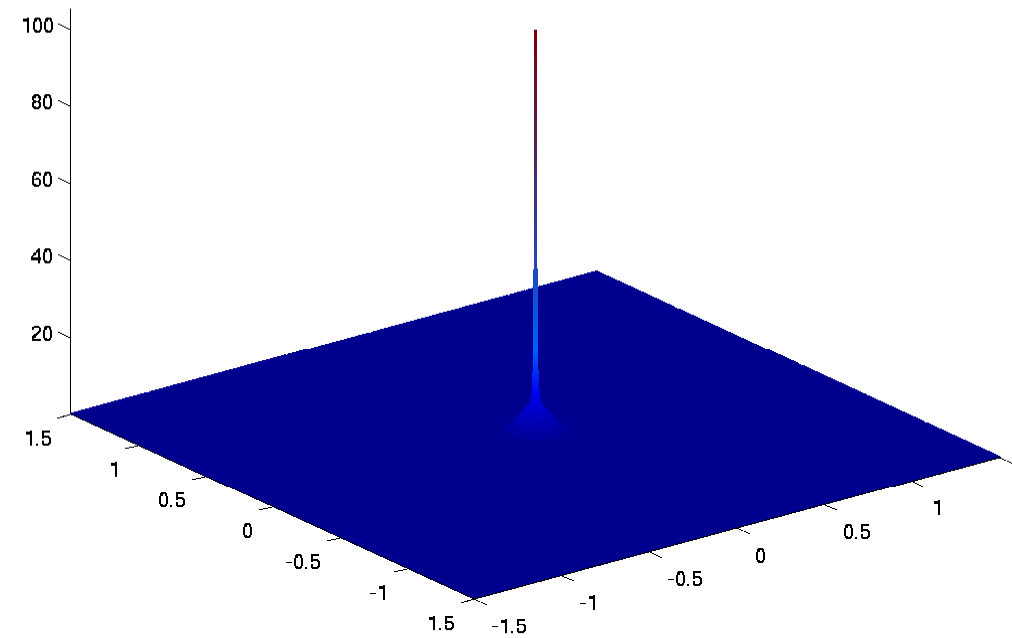
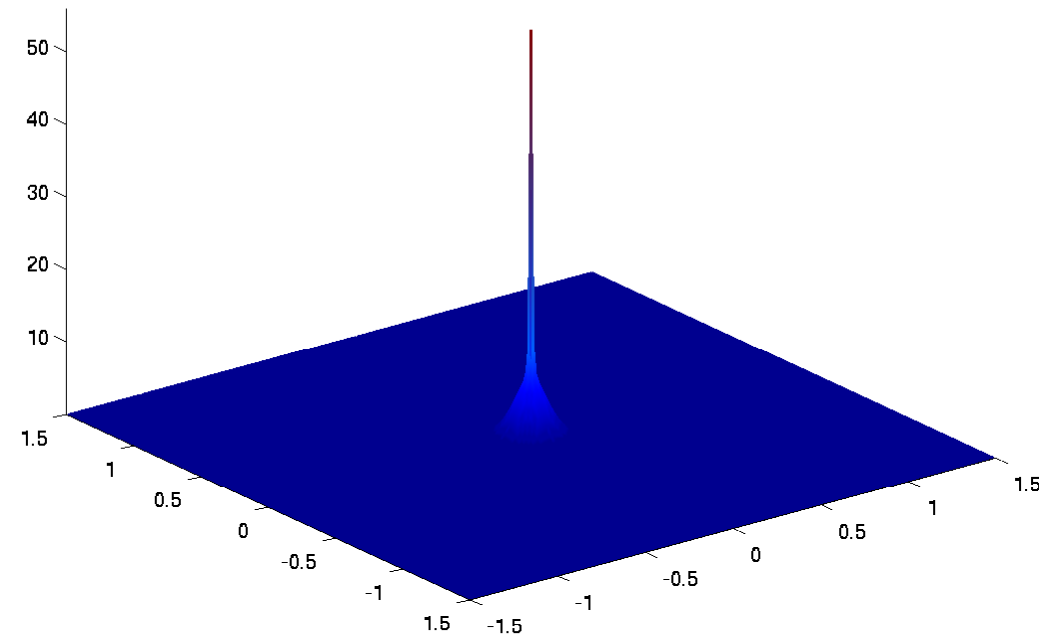
The magnitude of ρ_2 increases by a factor of about 4, which clearly indicates that by this time ρ_2 has already blown up:

$$\max_{j,k}(\rho_2)_{j,k} \sim \frac{1}{h^2}$$

200 × 200 vs. 400 × 400

ρ_1

ρ_1



ρ_1 increases only by a factor of about 2, which means that ρ_1 blows up at a lower rate (no δ -type singularity forms)

$$\max_{j,k}(\rho_1)_{j,k} \sim \frac{1}{h}$$

Example 3 — Different Types of Blow-Up of ρ_1 and ρ_2 in Region B

- Square domain $\Omega = [-3, 3] \times [-3, 3]$

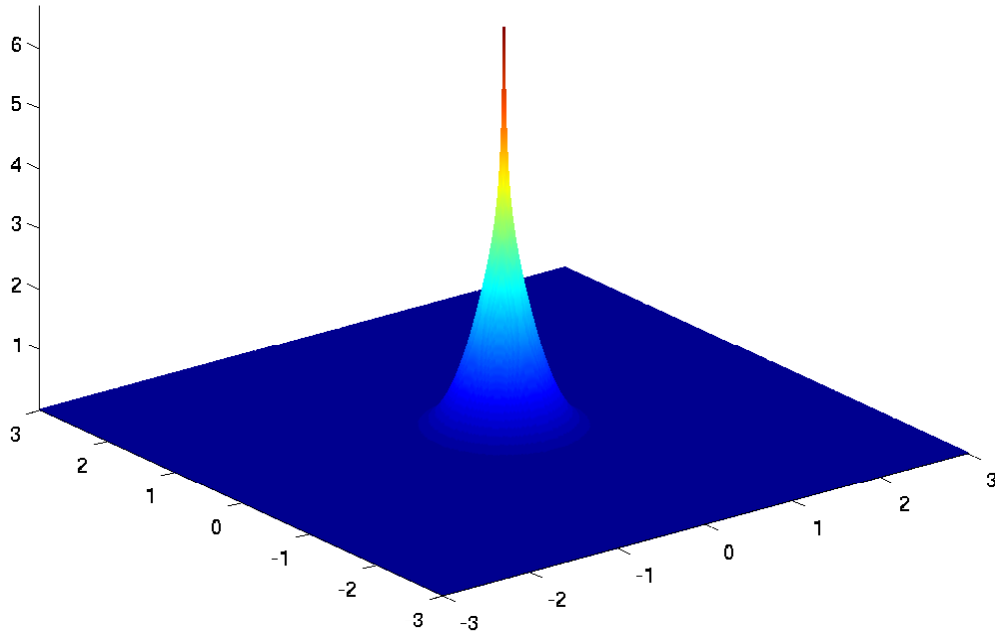
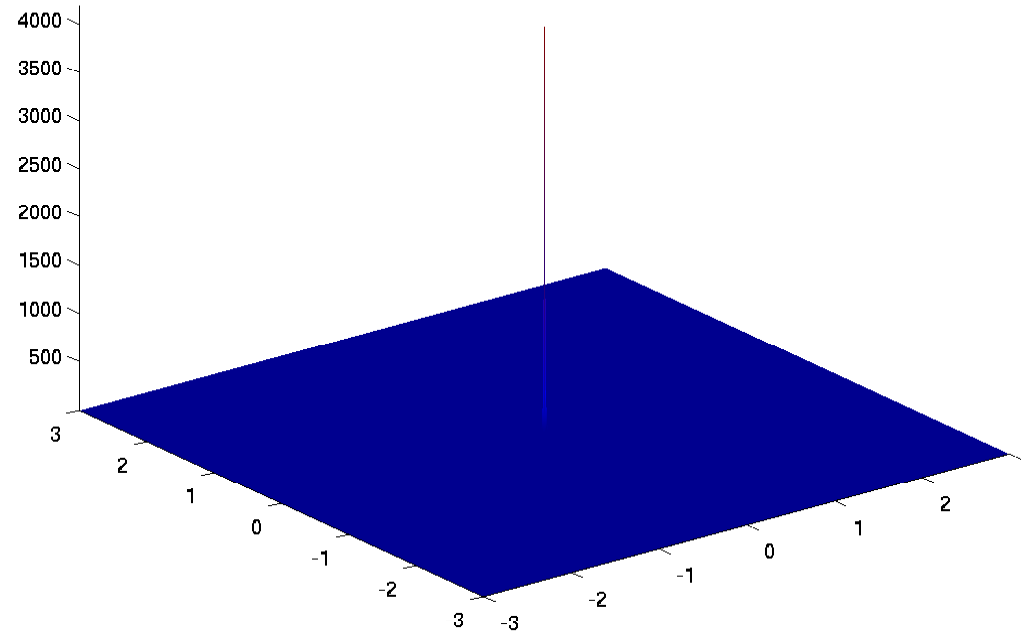
- Initial conditions:

$$\rho_1(x, y, 0) \equiv \rho_2(x, y, 0) = 50 e^{-100(x^2+y^2)}$$

- Parameters:

$$\chi_1 = 1, \quad \chi_2 = 20, \quad \mu_1 = 1$$

- Neumann boundary conditions

ρ_1  ρ_2 

This numerical experiment indicates that it is possible that in Region **B** one of the species aggregates and its density blows up, while the density of the second component remains bounded with decaying magnitude...

However...

However, this contradicts the analytical results, obtained for the above 2-species system in \mathbb{R}^2 .

We take a large square domain and use the Neumann boundary conditions, which are typically used to represent open boundary conditions on truncated computational domains. In none of the numerical examples, the solution behavior was affected by the boundary conditions, that is, all of the numerical solutions remain flat near the boundaries. This makes us to believe that the solution in \mathbb{R}^2 should behave similarly.

Q: How to explain the contradiction?

A: More careful numerical experiments show that:

The magnitude of ρ_2 increases by a factor of about 4, that is, ρ_2 develops a δ -type singularity:

$$\max_{j,k}(\rho_2)_{j,k} \sim \frac{1}{h^2}$$

while ρ_1 blows up at a very slow rate:

$$\max_{j,k}(\rho_1)_{j,k} \sim \frac{1}{h^{1/4}}$$

Numerical Challenge: How to compute such solutions?

Coupled Chemotaxis-Fluid Model

$$\begin{cases} n_t + \mathbf{u} \cdot \nabla n + \chi \nabla \cdot [nr(c)\nabla c] = D_n \Delta n \\ c_t + \mathbf{u} \cdot \nabla c = D_c \Delta c - n\kappa r(c) \\ \rho(\mathbf{u}_t + \mathbf{u} \cdot \nabla \mathbf{u}) + \nabla p = \eta \Delta \mathbf{u} - n \nabla \Phi \\ \nabla \cdot \mathbf{u} = 0 \end{cases}$$

n : concentration of bacteria

c : concentration of oxygen

χ : chemotactic sensitivity constant

\mathbf{u} : fluid velocity, ρ : density, p : pressure, η : viscosity

D_n and D_c : diffusion constants

$$\begin{cases} n_t + \mathbf{u} \cdot \nabla n + \chi \nabla \cdot [nr(c)\nabla c] = D_n \Delta n \\ c_t + \mathbf{u} \cdot \nabla c = D_c \Delta c - n\kappa r(c) \\ \rho(\mathbf{u}_t + \mathbf{u} \cdot \nabla \mathbf{u}) + \nabla p = \eta \Delta \mathbf{u} - n \nabla \Phi \\ \nabla \cdot \mathbf{u} = 0 \end{cases}$$

$\nabla \Phi := V_b g (\rho_b - \rho) \mathbf{z}$: gravitational force exerted by a bacterium onto the fluid;

\mathbf{z} : upwards unit vector, V_b : volume of the bacterium

$g = 9.8 \text{ m/s}^2$: gravitation acceleration

ρ_b : density of bacteria, which are about 10% denser than water

$r(c) = \theta(c - c^*)$: dimensionless cut-off function, which models an inactivity threshold of the bacteria due to low oxygen supply

$$\begin{cases} n_t + \mathbf{u} \cdot \nabla n + \chi \nabla \cdot [nr(c)\nabla c] = D_n \Delta n \\ c_t + \mathbf{u} \cdot \nabla c = D_c \Delta c - n\kappa r(c) \\ \rho(\mathbf{u}_t + \mathbf{u} \cdot \nabla \mathbf{u}) + \nabla p = \eta \Delta \mathbf{u} - n \nabla \Phi \\ \nabla \cdot \mathbf{u} = 0 \end{cases}$$

- Bacteria and oxygen are convected with fluid and diffuse
- Oxygen is consumed
- Bacteria are directed towards high oxygen gradient

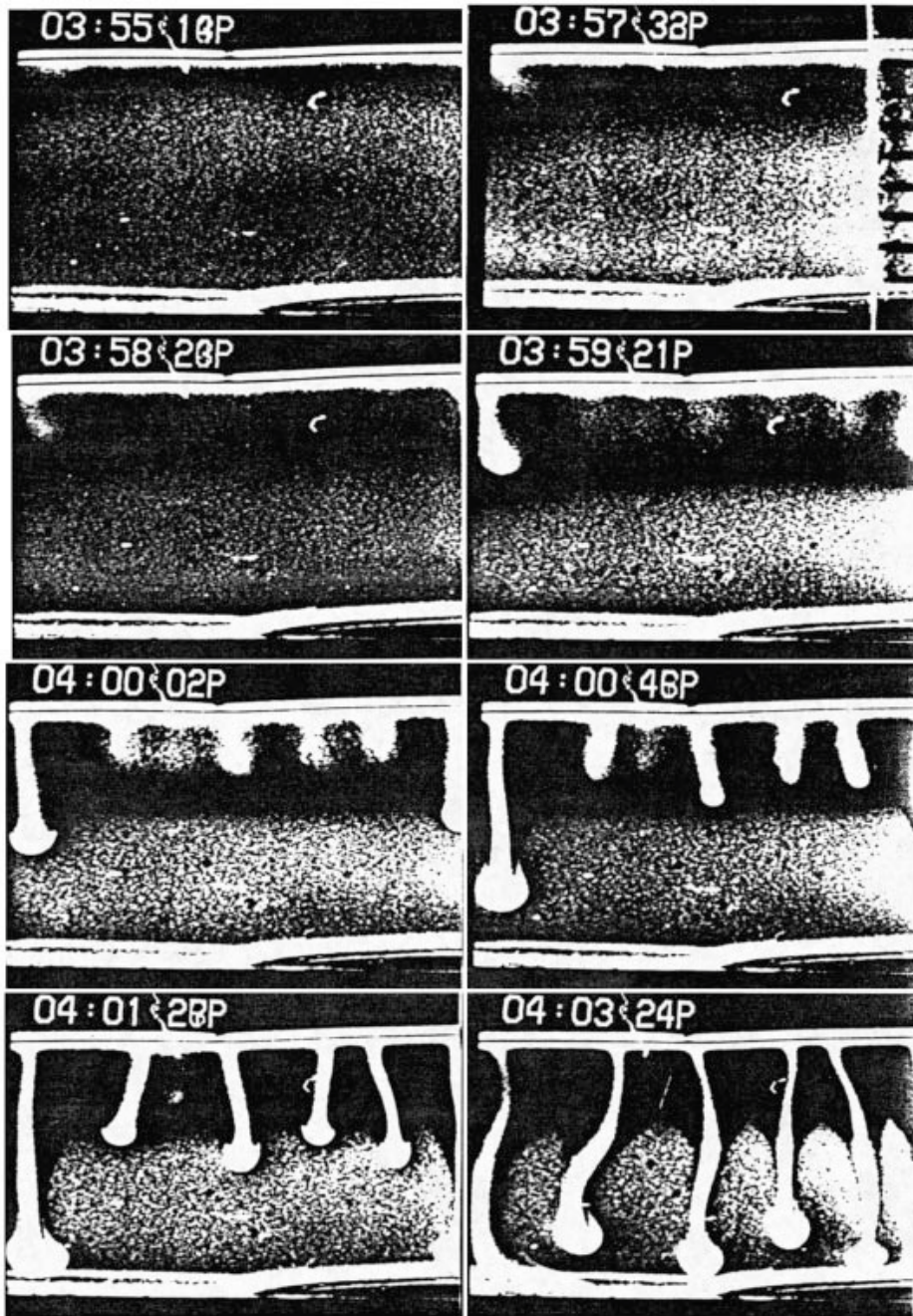
Bioconvection

Bioconvection is the spontaneous formation of patterns in suspensions of swimming micro-organisms

Organisms exhibiting bioconvection have two things in common: they are denser than water; they swim upwards in still water.

Example: Complex bioconvection patterns are observed when a (well-stirred) suspension of bacterial cells (e.g. *Bacillus subtilis*) is placed in a chamber with its upper surface open to the atmosphere.

- The cells are **aerotactic**
- Upswimming causes the micro-organisms to accumulate in the upper regions of the fluid
- This distribution is **unstable** since the cells are denser than water
- The instability leads to the formation of patterns in the form of **descending plumes**



The initial suspension of of the aerobic bacteria *B. subtilis* is well stirred and quasi-homogeneous.

- A **high concentration layer** forms near the surface as cell swim up following the oxygen gradient
- **Instabilities** form at this layer and **finger-shaped plumes** begin to sink downwards
- Turn into **mushroom-shaped plumes** in the areas where the oxygen concentration is below the aerotaxis threshold

Non-dimensionalization and switching to vorticity formulation:

$$\begin{cases} n_t + \operatorname{div}(\mathbf{u}n) + \alpha \nabla \cdot [r(c)n \nabla c] = \Delta n \\ c_t + \operatorname{div}(\mathbf{u}c) = \delta \Delta c - \beta r(c)n \\ \omega_t + \operatorname{div}(\mathbf{u}\omega) = Sc \Delta \omega - \gamma Sc n_x \\ \Delta \psi = -\omega \end{cases}$$

$\omega := v_x - u_y$: vorticity, ψ : stream-function, $u = \psi_y$, $v = -\psi_x$

Initial Conditions in $\Omega = [-a, a] \times [0, d]$:

$$n(x, y, 0) = n_0(x, y), \quad c(x, y, 0) = c_0(x, y), \quad \mathbf{u}(x, y, 0) = \mathbf{u}_0(x, y)$$

Boundary Conditions in $\Omega = [-a, a] \times [0, d]$:

$$\alpha r(c)nc_y - n_y = 0, \quad c = 1, \quad v = 0, \quad u_y = 0, \quad \forall (x, y) : y = d$$

$$n_y = c_y = 0, \quad u = v = 0, \quad \forall (x, y) : y = 0$$

At the sides of Ω ($x = \pm a$) the boundary conditions are periodic

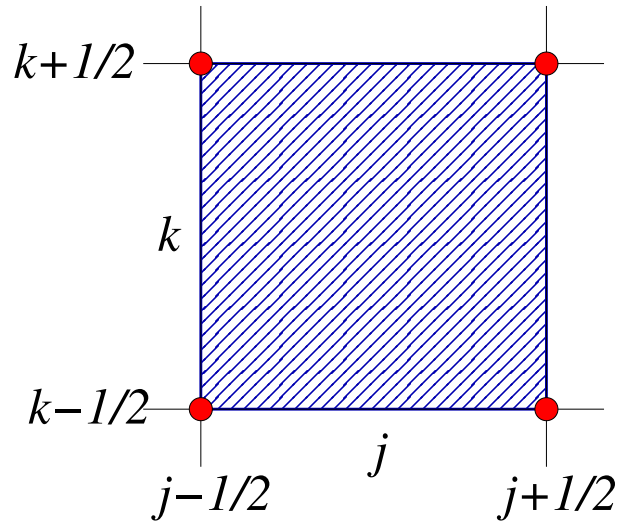
Hybrid Finite-Volume Finite-Difference Scheme

$$\begin{cases} n_t + [(u + \alpha r(c)c_x)n]_x + [(v + \alpha r(c)c_y)n]_y = n_{xx} + n_{yy}, \\ c_t + (uc)_x + (vc)_y = \delta(c_{xx} + c_{yy}) - \beta r(c)n \\ \omega_t + u\omega_x + v\omega_y = SC(\omega_{xx} + \omega_{yy}) - \gamma SC n_x, \\ \psi_{xx} + \psi_{yy} = -\omega. \end{cases}$$

- n and c are evolved in time by solving the chemotaxis equations using the second-order **finite-volume upwind method**
- ω is evolved on a staggered grid by applying the second-order **centered-difference scheme** to the vorticity equation
- u and v are recovered from the stream-function ψ by solving the elliptic equation followed by the centered-difference approximations of the velocities in $u = \psi_y$ and $v = -\psi_x$

IMPORTANT: The scheme must be positivity preserving!

Finite-Volume Upwind Scheme



We denote the cell averages of $\mathbf{q} := (n, c)^T$ by

$$\bar{\mathbf{q}}_{j,k}(t) := \frac{1}{\Delta x \Delta y} \iint_{C_{j,k}} \mathbf{q}(x, y, t) dx dy$$

$$\begin{aligned} \iint_{C_{j,k}} n_t + \iint_{C_{j,k}} [(u + \alpha r(c)c_x)n]_x + \iint_{C_{j,k}} [(v + \alpha r(c)c_y)n]_y &= \iint_{C_{j,k}} (n_{xx} + n_{yy}) \\ \iint_{C_{j,k}} c_t + \iint_{C_{j,k}} (uc)_x + \iint_{C_{j,k}} (vc)_y &= \iint_{C_{j,k}} \delta(c_{xx} + c_{yy}) - \iint_{C_{j,k}} \beta r(c)n \end{aligned}$$

$$\frac{d}{dt} \bar{n}_{j,k} \approx - \frac{(u + \alpha r(c)c_x)n \Big|_{(x_{j+\frac{1}{2}}, y_k)} - (u + \alpha r(c)c_x)n \Big|_{(x_{j-\frac{1}{2}}, y_k)}}{\Delta x} - \frac{(v + \alpha r(c)c_y)n \Big|_{(x_j, y_{k+\frac{1}{2}})} - (v + \alpha r(c)c_y)n \Big|_{(x_j, y_{k-\frac{1}{2}})}}{\Delta y} + \frac{n_x \Big|_{(x_{j+\frac{1}{2}}, y_k)} - n_x \Big|_{(x_{j-\frac{1}{2}}, y_k)}}{\Delta x} + \frac{n_y \Big|_{(x_j, y_{k+\frac{1}{2}})} - n_y \Big|_{(x_j, y_{k-\frac{1}{2}})}}{\Delta y}$$

$$\frac{d}{dt} \bar{c}_{j,k} \approx - \frac{uc \Big|_{(x_{j+\frac{1}{2}}, y_k)} - uc \Big|_{(x_{j-\frac{1}{2}}, y_k)}}{\Delta x} - \frac{vc \Big|_{(x_j, y_{k+\frac{1}{2}})} - vc \Big|_{(x_j, y_{k-\frac{1}{2}})}}{\Delta y} + \delta \frac{c_x \Big|_{(x_{j+\frac{1}{2}}, y_k)} - c_x \Big|_{(x_{j-\frac{1}{2}}, y_k)}}{\Delta x} + \delta \frac{c_y \Big|_{(x_j, y_{k+\frac{1}{2}})} - c_y \Big|_{(x_j, y_{k-\frac{1}{2}})}}{\Delta y} + \beta r(\bar{c}_{j,k}) \bar{n}_{j,k}$$

Semi-Discrete Finite-Volume Upwind Scheme

$$\frac{d}{dt} \bar{\mathbf{q}}_{j,k} = - \frac{\mathbf{H}^x_{j+\frac{1}{2},k} - \mathbf{H}^x_{j-\frac{1}{2},k}}{\Delta x} - \frac{\mathbf{H}^y_{j,k+\frac{1}{2}} - \mathbf{H}^y_{j,k-\frac{1}{2}}}{\Delta y} + \frac{\mathbf{P}^x_{j+\frac{1}{2},k} - \mathbf{P}^x_{j-\frac{1}{2},k}}{\Delta x} + \frac{\mathbf{P}^y_{j,k+\frac{1}{2}} - \mathbf{P}^y_{j,k-\frac{1}{2}}}{\Delta y} + \bar{\mathbf{R}}_{j,k},$$

$$\mathbf{H}^x_{j\pm\frac{1}{2},k} \approx \left((u + \alpha r(c)c_x)n \Big|_{(x_{j\pm\frac{1}{2}}, y_k)}, u c \Big|_{(x_{j\pm\frac{1}{2}}, y_k)} \right)^T$$

$$\mathbf{H}^y_{j,k\pm\frac{1}{2}} \approx \left((v + \alpha r(c)c_y)n \Big|_{(x_j, y_{k\pm\frac{1}{2}})}, v c \Big|_{(x_j, y_{k\pm\frac{1}{2}})} \right)^T$$

$$\mathbf{P}^x_{j\pm\frac{1}{2},k} \approx \left(n_x \Big|_{(x_{j\pm\frac{1}{2}}, y_k)}, \delta c_x \Big|_{(x_{j\pm\frac{1}{2}}, y_k)} \right)^T$$

$$\mathbf{P}^y_{j,k\pm\frac{1}{2}} \approx \left(n_y \Big|_{(x_j, y_{k\pm\frac{1}{2}})}, c_y \Big|_{(x_j, y_{k\pm\frac{1}{2}})} \right)^T, \quad \bar{\mathbf{R}}_{j,k} = (0, \beta r(\bar{c}_{j,k}) \bar{n}_{j,k})^T$$

Hyperbolic Fluxes

$$\mathbf{H}_{j\pm\frac{1}{2},k}^x \approx \left((u + \alpha r(c)c_x) n \Big|_{(x_{j\pm\frac{1}{2}}, y_k)}, u c \Big|_{(x_{j\pm\frac{1}{2}}, y_k)} \right)^T$$

$$\mathbf{H}_{j,k\pm\frac{1}{2}}^y \approx \left((v + \alpha r(c)c_y) n \Big|_{(x_j, y_{k\pm\frac{1}{2}})}, v c \Big|_{(x_j, y_{k\pm\frac{1}{2}})} \right)^T$$

$$\mathbf{H}_{j+\frac{1}{2},k}^{x,(i)} = \begin{cases} a_{j+\frac{1}{2},k}^{(i)} \mathbf{q}_{j,k}^{E,(i)}, & \text{if } a_{j+\frac{1}{2},k}^{(i)} > 0, \\ a_{j+\frac{1}{2},k}^{(i)} \mathbf{q}_{j+1,k}^{W,(i)}, & \text{if } a_{j+\frac{1}{2},k}^{(i)} < 0, \end{cases} \quad i = 1, 2$$

$$\mathbf{H}_{j,k+\frac{1}{2}}^{y,(i)} = \begin{cases} b_{j,k+\frac{1}{2}}^{(i)} \mathbf{q}_{j,k}^{N,(i)}, & \text{if } b_{j,k+\frac{1}{2}}^{(i)} > 0, \\ b_{j,k+\frac{1}{2}}^{(i)} \mathbf{q}_{j,k+1}^{S,(i)}, & \text{if } b_{j,k+\frac{1}{2}}^{(i)} < 0, \end{cases} \quad i = 1, 2$$

Local speeds:

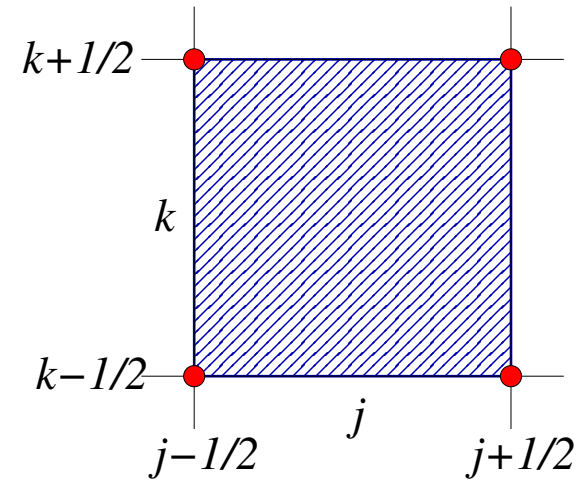
$$a_{j+\frac{1}{2},k}^{(1)} = u_{j+\frac{1}{2},k} + \alpha r(c_{j+\frac{1}{2},k})(c_x)_{j+\frac{1}{2},k}, \quad a_{j+\frac{1}{2},k}^{(2)} = u_{j+\frac{1}{2},k}$$

$$b_{j,k+\frac{1}{2}}^{(1)} = v_{j,k+\frac{1}{2}} + \alpha r(c_{j,k+\frac{1}{2}})(c_y)_{j,k+\frac{1}{2}}, \quad b_{j,k+\frac{1}{2}}^{(2)} = v_{j,k+\frac{1}{2}}$$

Parabolic Fluxes

$$\mathbf{P}_{j\pm\frac{1}{2},k}^x \approx \left(n_x \Big|_{(x_{j\pm\frac{1}{2}}, y_k)}, \delta c_x \Big|_{(x_{j\pm\frac{1}{2}}, y_k)} \right)^T$$

$$\mathbf{P}_{j,k\pm\frac{1}{2}}^y \approx \left(n_y \Big|_{(x_j, y_{k\pm\frac{1}{2}})}, \delta c_y \Big|_{(x_j, y_{k\pm\frac{1}{2}})} \right)^T$$



$$\mathbf{P}_{j+\frac{1}{2},k}^x = \left(\frac{\bar{n}_{j+1,k} - \bar{n}_{j,k}}{\Delta x}, \delta \frac{\bar{c}_{j+1,k} - \bar{c}_{j,k}}{\Delta x} \right)^T$$

$$\mathbf{P}_{j,k+\frac{1}{2}}^y = \left(\frac{\bar{n}_{j,k+1} - \bar{n}_{j,k}}{\Delta y}, \delta \frac{\bar{c}_{j,k+1} - \bar{c}_{j,k}}{\Delta y} \right)^T$$

Centered-Difference Scheme for the Vorticity Equation

$$\omega_t + u\omega_x + v\omega_y = Sc(\omega_{xx} + \omega_{yy}) - \gamma Sc n_x,$$

$$\psi_{xx} + \psi_{yy} = -\omega.$$

Evolve the point values of ω at the corners of the finite-volume cells:

$$\begin{aligned} \frac{d}{dt}\omega_{j+\frac{1}{2},k+\frac{1}{2}} = & -u_{j+\frac{1}{2},k+\frac{1}{2}} \frac{\omega_{j+\frac{3}{2},k+\frac{1}{2}} - \omega_{j-\frac{1}{2},k+\frac{1}{2}}}{2\Delta x} - v_{j+\frac{1}{2},k+\frac{1}{2}} \frac{\omega_{j+\frac{1}{2},k+\frac{3}{2}} - \omega_{j+\frac{1}{2},k-\frac{1}{2}}}{2\Delta y} \\ & + Sc \left[\frac{\omega_{j+\frac{3}{2},k+\frac{1}{2}} - 2\omega_{j+\frac{1}{2},k+\frac{1}{2}} + \omega_{j-\frac{1}{2},k+\frac{1}{2}}}{(\Delta x)^2} + \frac{\omega_{j+\frac{1}{2},k+\frac{3}{2}} - 2\omega_{j+\frac{1}{2},k+\frac{1}{2}} + \omega_{j+\frac{1}{2},k-\frac{1}{2}}}{(\Delta y)^2} \right] \\ & - \gamma Sc (n_x)_{j+\frac{1}{2},k+\frac{1}{2}} \end{aligned}$$

$(n_x)_{j+\frac{1}{2},k+\frac{1}{2}}$ is computed by the centered-difference formula

$$(n_x)_{j+\frac{1}{2},k+\frac{1}{2}} = \frac{(n_{j+1,k}^N + n_{j+1,k+1}^S) - (n_{j,k}^N + n_{j,k+1}^S)}{2\Delta x}$$

Velocities

Once the point values of the vorticity $\{\omega_{j+\frac{1}{2},k+\frac{1}{2}}\}$ are evolved

- Solve the elliptic equation

$$\psi_{xx} + \psi_{yy} = -\omega$$

- Obtain the point values of the stream-function at the same set of points: $\{\psi_{j+\frac{1}{2},k+\frac{1}{2}}\}$

- Compute the velocities u and v :

$$u_{j+\frac{1}{2},k+\frac{1}{2}} = \frac{\psi_{j+\frac{1}{2},k+\frac{3}{2}} - \psi_{j+\frac{1}{2},k-\frac{1}{2}}}{2\Delta y}, \quad v_{j+\frac{1}{2},k+\frac{1}{2}} = -\frac{\psi_{j+\frac{3}{2},k+\frac{1}{2}} - \psi_{j-\frac{1}{2},k+\frac{1}{2}}}{2\Delta x}$$
$$u_{j+\frac{1}{2},k} = \frac{\psi_{j+\frac{1}{2},k+\frac{1}{2}} - \psi_{j+\frac{1}{2},k-\frac{1}{2}}}{\Delta y}, \quad v_{j,k+\frac{1}{2}} = -\frac{\psi_{j+\frac{1}{2},k+\frac{1}{2}} - \psi_{j-\frac{1}{2},k+\frac{1}{2}}}{\Delta x}$$

Boundary Conditions

Computational domain: $\Omega = [-a, a] \times [0, d]$

- The top part $\partial\Omega_{top}$ models a fluid-air surface preventing cell-flux and providing full oxygen saturation:

$$\alpha r(c)nc_y - n_y = 0, \quad c = 1, \quad \omega = 0, \quad \psi = 0, \quad \forall(x, y) : y = d$$

- The bottom part $\partial\Omega_{bot}$ model a solid bottom preventing cell- and oxygen-flux:

$$n_y = c_y = 0, \quad \psi_y = 0, \quad \omega = -\psi_{yy}, \quad \forall(x, y) : y = 0$$

- At the sides of Ω_{side} ($x = \pm a$) the boundary conditions are periodic.

Note that the Poisson equation implies $\psi_{xx} = 0$ at the lower boundary $y = 0$, which together with the periodicity and continuity gives $\psi = \text{Const}$ at $y = 0$. Thus, $v = 0$ at $y = 0$ follows.

Numerical Boundary Conditions

- The top part $\partial\Omega_{top}$:

$$\bar{n}_{j,k_{\max}+1} := \bar{n}_{j,k_{\max}} e^{\alpha(1-\bar{c}_{j,k_{\max}})}, \quad \bar{c}_{j,k_{\max}+1} = 1$$

$$\omega_{j+\frac{1}{2},k_{\max}+\frac{1}{2}} = \psi_{j+\frac{1}{2},k_{\max}+\frac{1}{2}} = 0$$

where the boundary condition for n is obtained by taking into account the fact that at the top $c \sim 1$ and thus $r(c) = 1$ and by integrating $(\ln n)_y = \alpha c_y$ with respect to y from $y_{k_{\max}}$ to $y_{k_{\max}+1}$

- The bottom part $\partial\Omega_{bot}$:

$$\bar{n}_{j,0} := \bar{n}_{j,1}, \quad \bar{c}_{j,0} = \bar{c}_{j,1}$$

$$\omega_{j+\frac{1}{2},\frac{1}{2}} = -2 \frac{\psi_{j+\frac{1}{2},\frac{3}{2}} - \psi_{j+\frac{1}{2},\frac{1}{2}}}{(\Delta y)^2}, \quad \psi_{j+\frac{1}{2},-\frac{1}{2}} = \psi_{j+\frac{1}{2},\frac{3}{2}}$$

- The two sides $\partial\Omega_{side}$ are connected with periodic boundary conditions

Numerical Experiments

$$n_t + \operatorname{div}(\mathbf{u}n) + \alpha \nabla \cdot [r(c)n \nabla c] = \Delta n$$

$$c_t + \operatorname{div}(\mathbf{u}c) = \delta \Delta c - \beta r(c)n$$

$$\omega_t + \operatorname{div}(\mathbf{u}\omega) = Sc \Delta \omega - \gamma Sc n_x$$

$$\Delta \psi = -\omega$$

Computational domain: $\Omega = [-3, 3] \times [0, 1]$

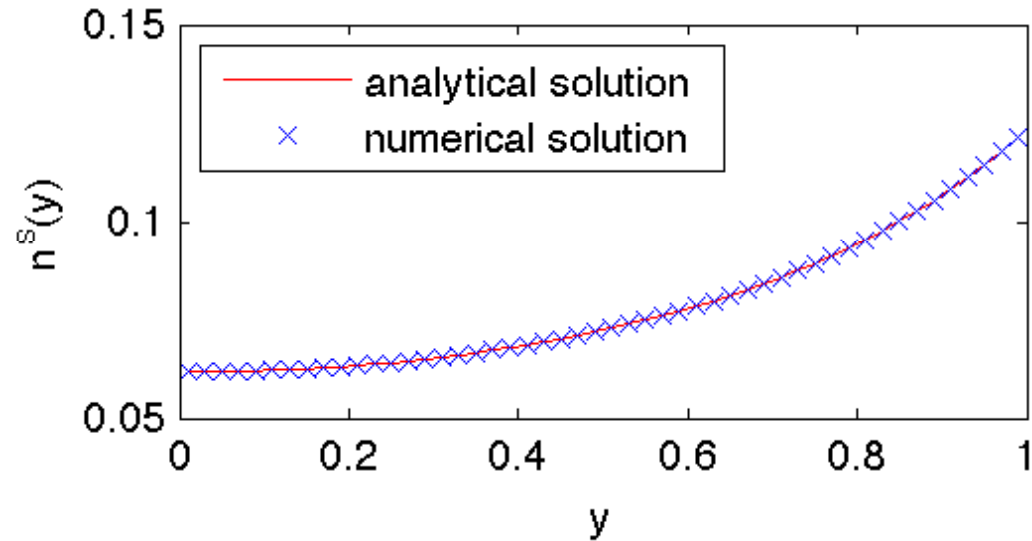
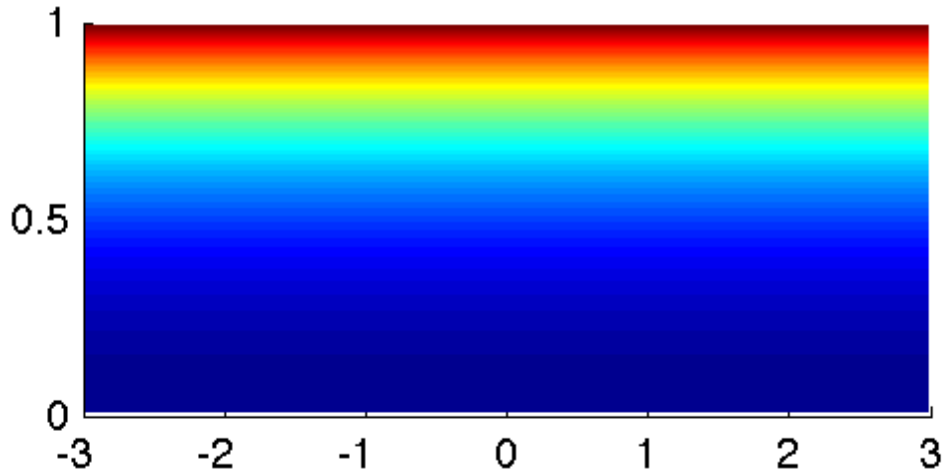
Parameters set by the model: $\alpha = 10$, $\delta = 5$, $Sc = 500$

Cutoff function $r(c)$, which modulates the oxygen consumption rate:

$$r(c) = \begin{cases} 1, & \text{if } c \geq 0.3, \\ 0, & \text{if } c < 0.3. \end{cases}$$

The numerical examples will vary the initial data and the two remaining parameters β and γ

Steady-States Solutions



$$\beta = 10, \quad \gamma = 10^3$$

The constant initial data are

$$n_0(x, y) \equiv \frac{\pi}{40}, \quad c_0(x, y) \equiv 1, \quad \mathbf{u}_0(x, y) \equiv \mathbf{0}$$

Plume Formation and Merging Plumes: Randomly Perturbed Homogeneous Initial Data

$$n_t + \text{div}(\mathbf{u}n) + \alpha \nabla \cdot [r(c)n \nabla c] = \Delta n$$

$$c_t + \text{div}(\mathbf{u}c) = \delta \Delta c - \beta r(c)n$$

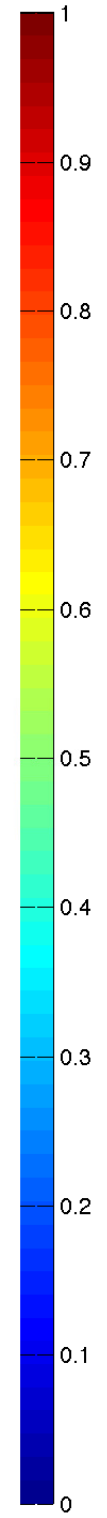
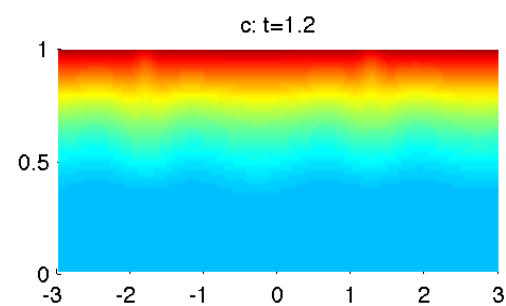
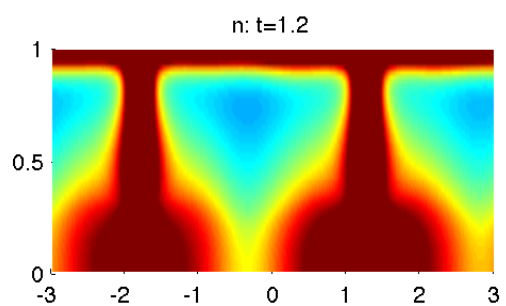
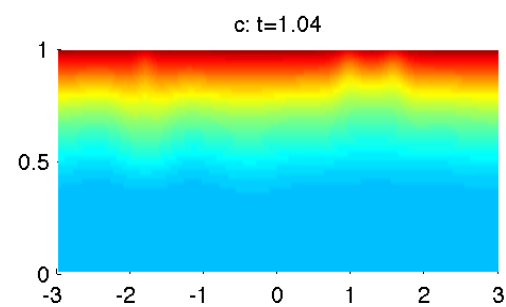
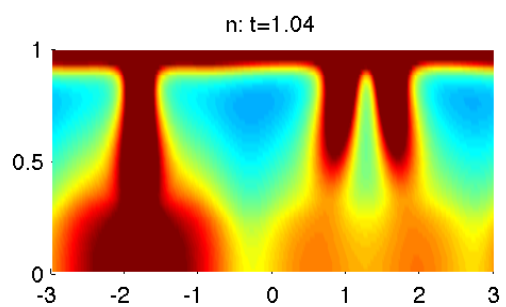
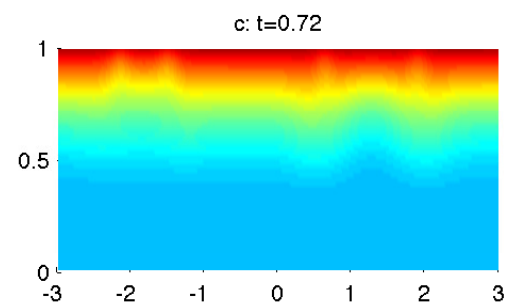
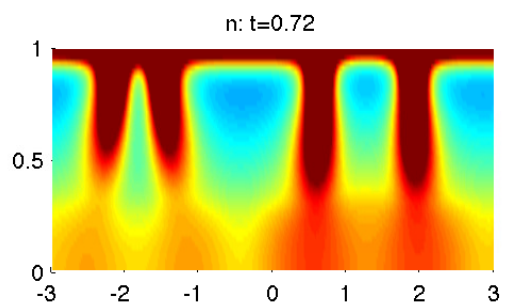
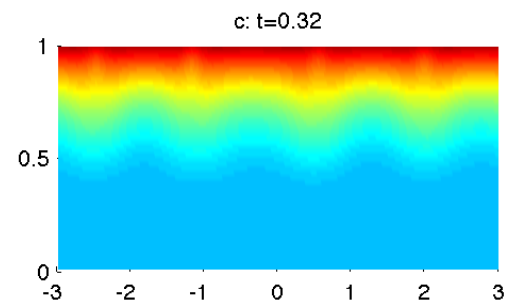
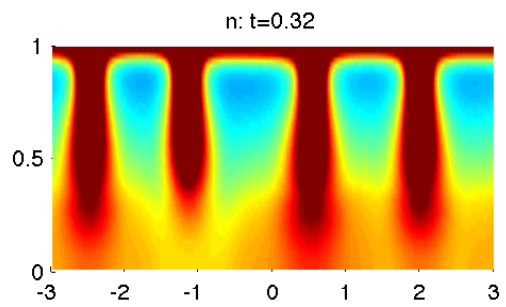
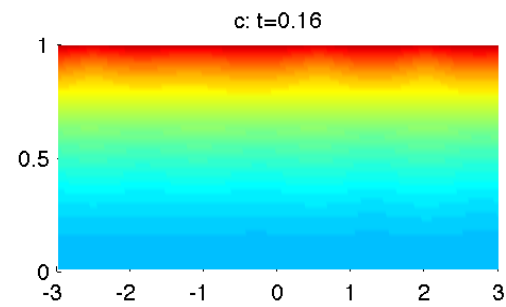
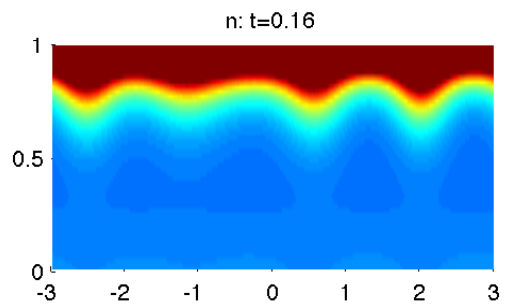
$$\omega_t + \text{div}(\mathbf{u}\omega) = Sc \Delta \omega - \gamma Sc n_x,$$

$$\Delta \psi = -\omega.$$

- $\beta = 20$ and $\gamma = 2 \cdot 10^3$, which corresponds to a doubled reference density compared to the homogeneous stationary state
- Initial data:

$$n_0(x, y) = 0.8 + 0.2\xi, \quad c_0(x, y) \equiv 1, \quad \mathbf{u}_0(x, y) \equiv \mathbf{0}$$

where ξ is a random variable uniformly distributed in the interval $[0, 1]$



Numerically Nonlinearly Stable Stationary Plumes for Low Density Initial Data

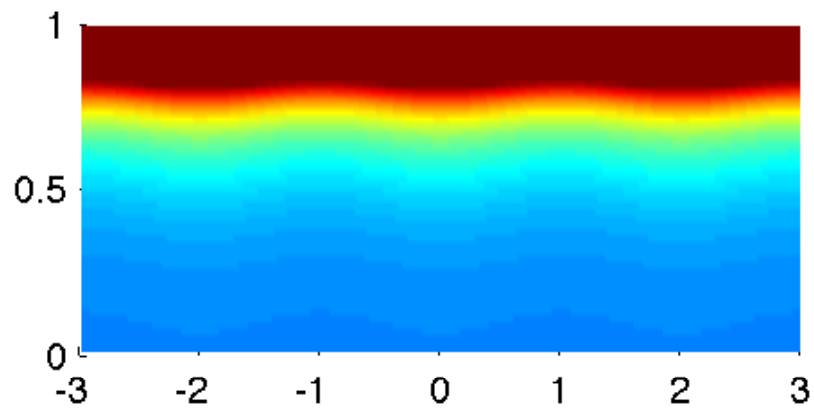
- Same parameters $\beta = 10, \gamma = 10^3$ as for the homogeneous stationary state
- Deterministic initial data (small, sinusoidal modulations of the lower edge of an upper layer with a higher cell concentration than at the bottom):

$$n_0(x, y) = \begin{cases} 1, & \text{if } y > 0.499 - 0.01 \sin((x - 1.5)\pi) \\ 0.5, & \text{otherwise} \end{cases}$$

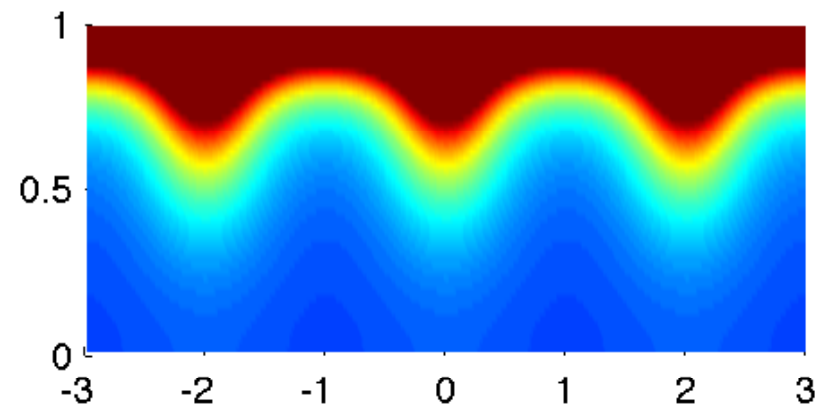
$$c_0(x, y) \equiv 1, \quad \mathbf{u}_0(x, y) \equiv \mathbf{0}$$

We study the time evolution of solutions from purely deterministic initial data towards a stationary state of plumes in the absence of oxygen cut-off (this case is referred to as the shallow-chamber case).

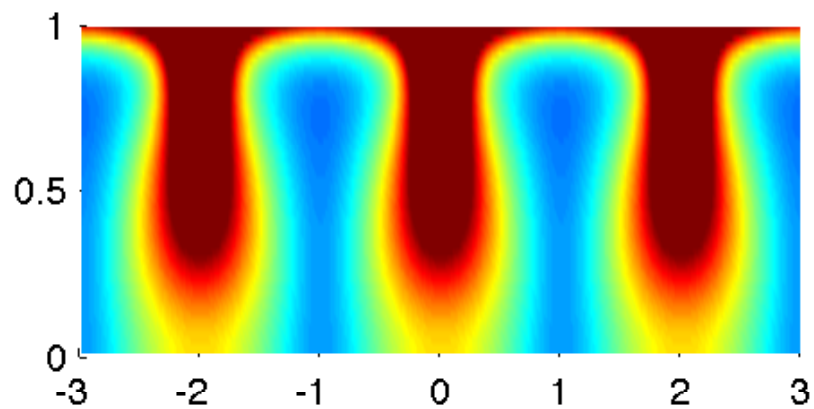
n: t=0.2



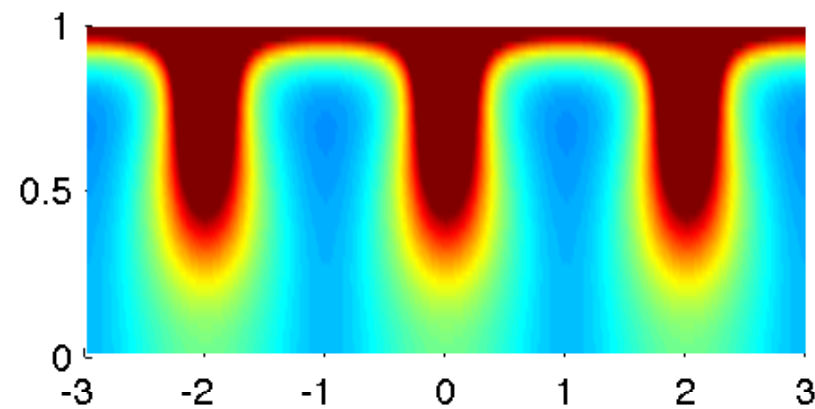
n: t=0.3



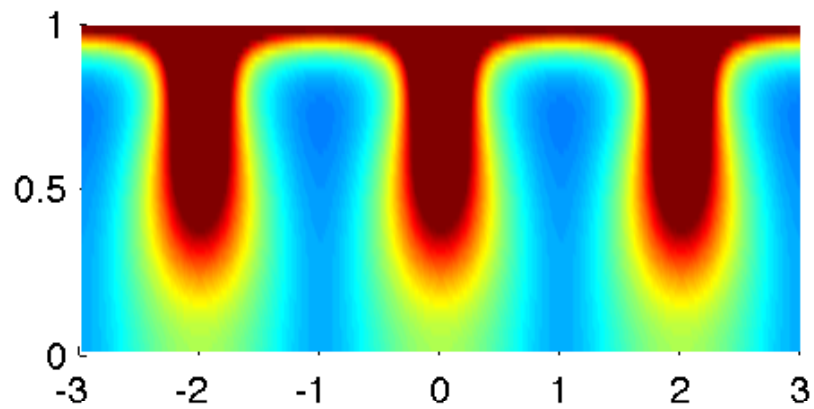
n: t=0.4



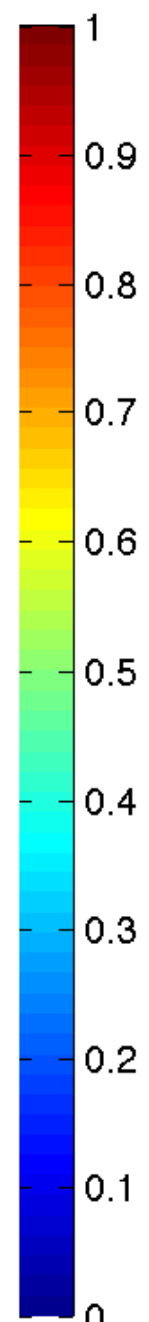
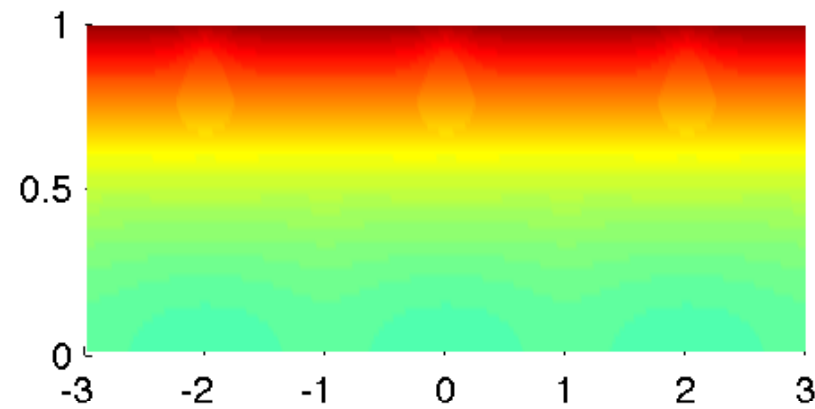
n: t=0.5

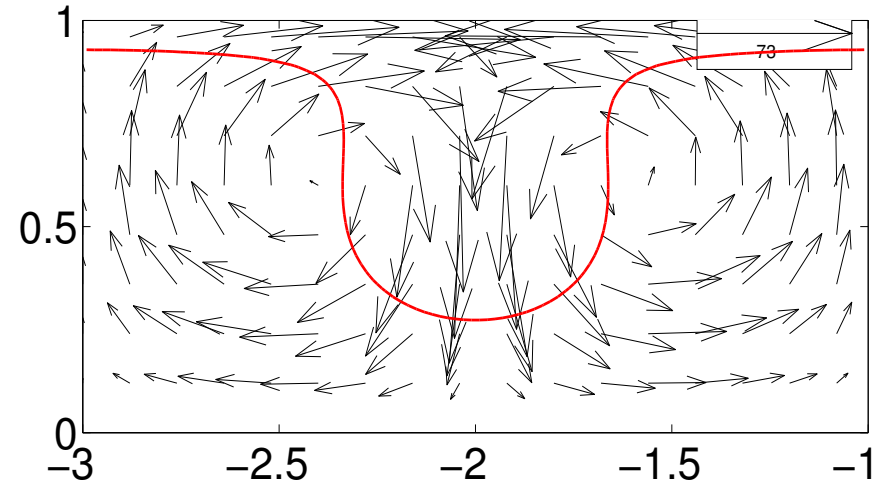
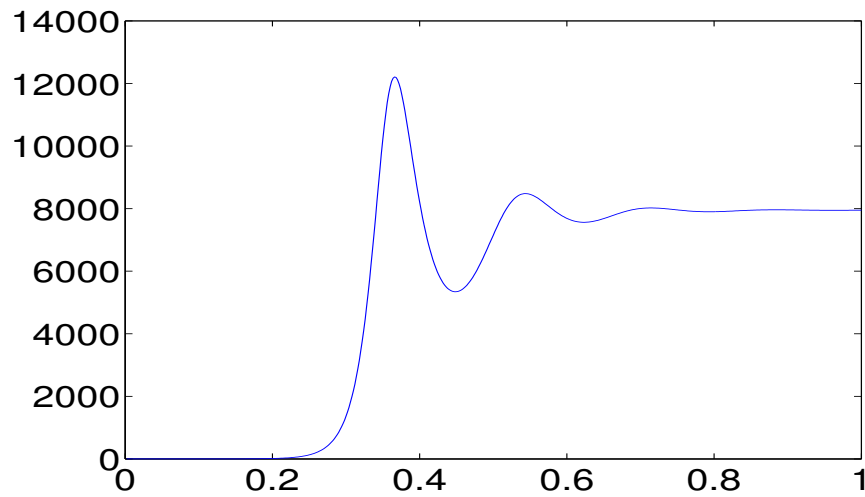


n: t=1

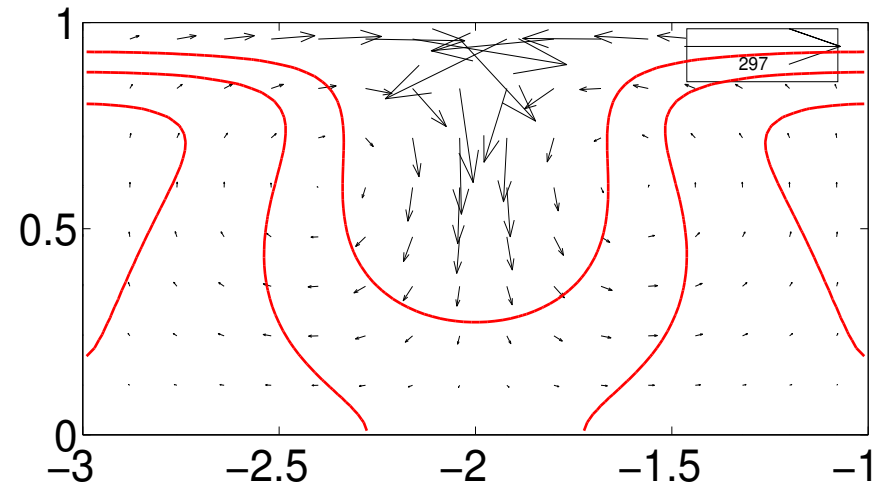
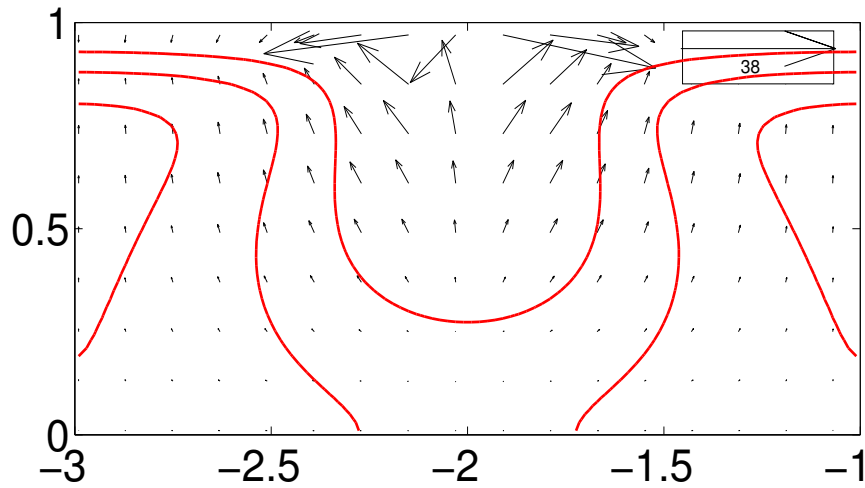


c: t=0.5



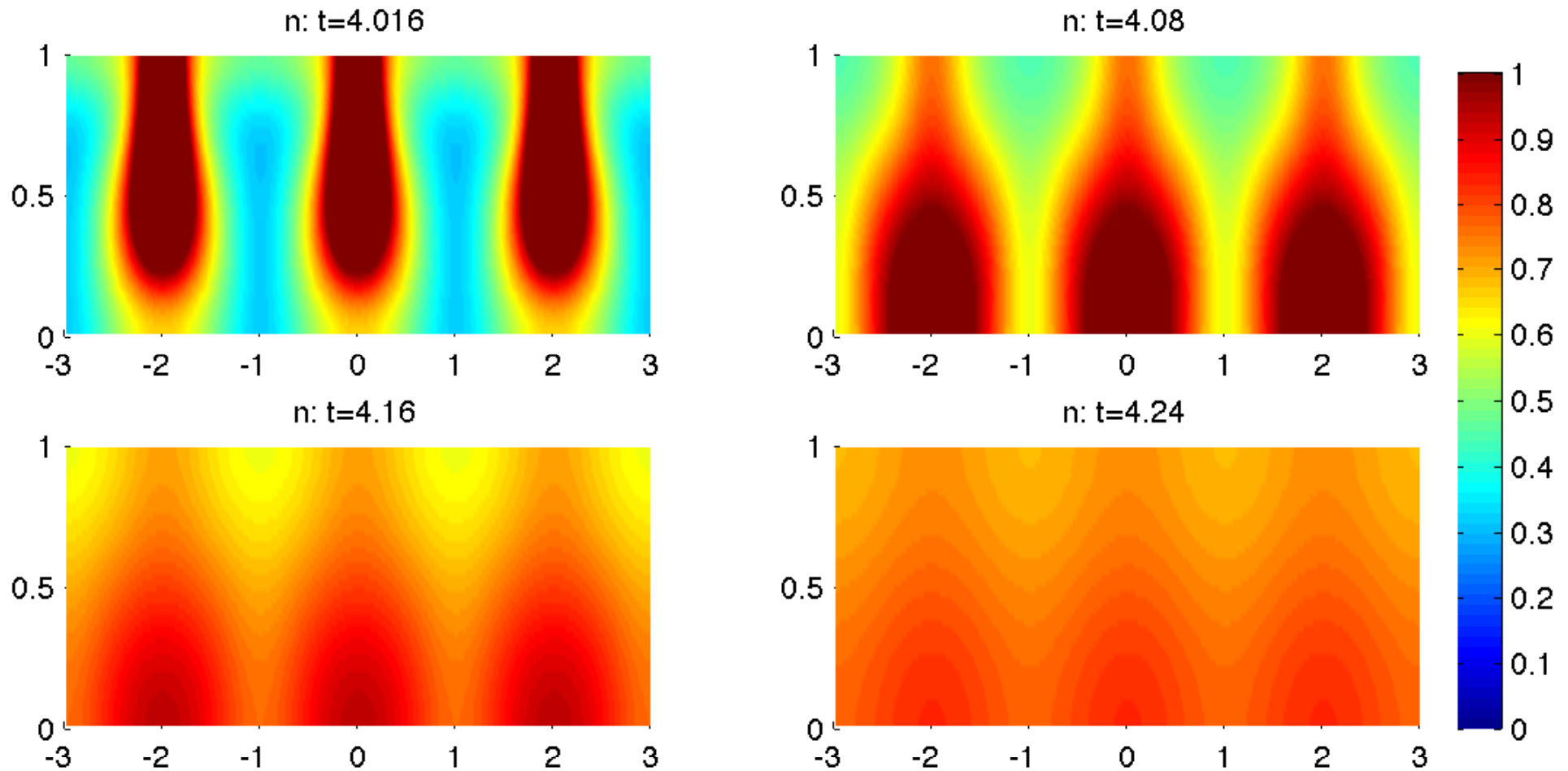


Time-evolution of kinetic energy (left). Velocity field \mathbf{u} (right).

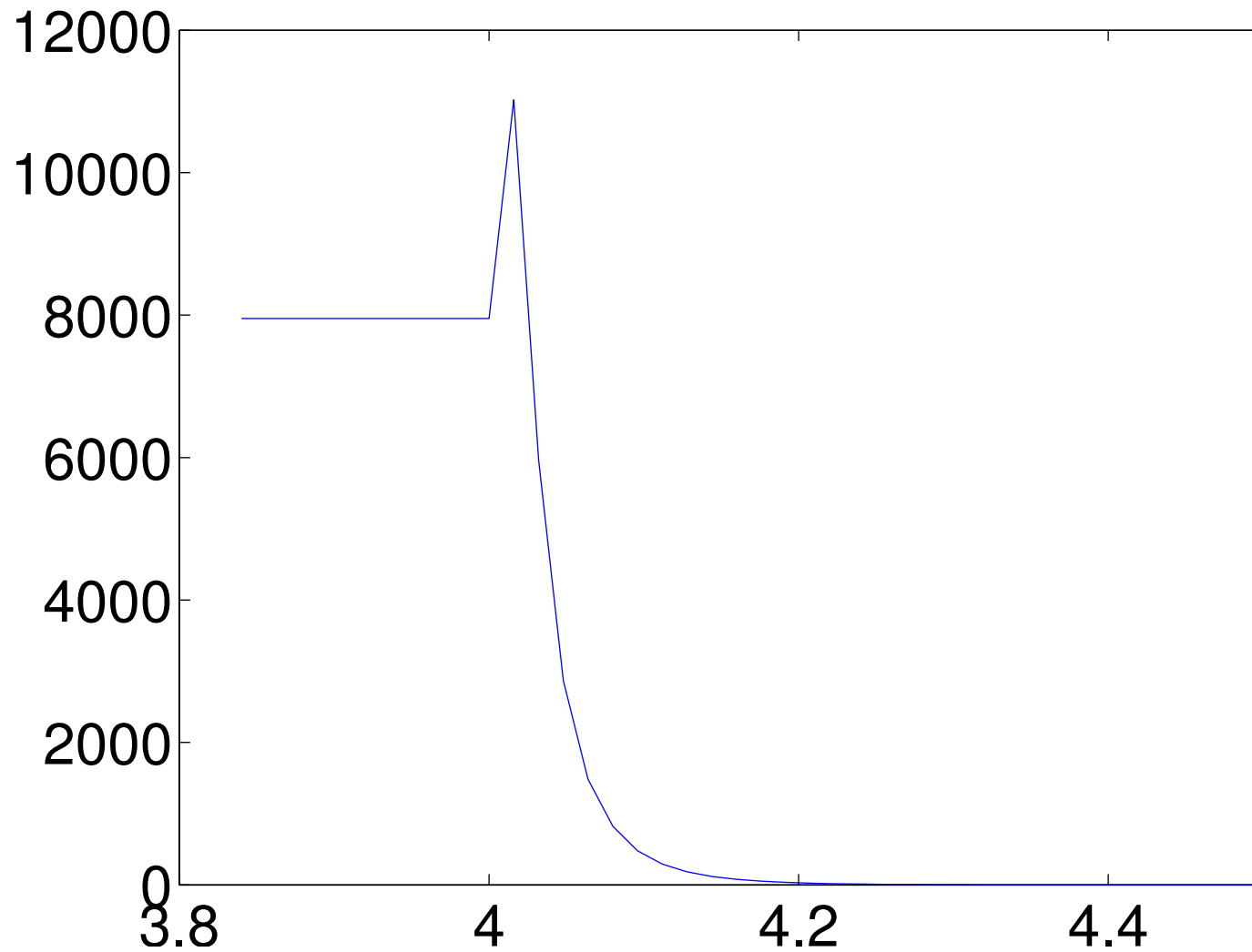


Aerotaxis/diffusion-component of the cell-flux $-\nabla n + \alpha n \nabla c$ (left). Fluid-driven cell-flux $\mathbf{u}n$ (right).

Switching-off Aerotaxis



Depletion of the high cell-concentration layer near the surface and diffusion of the plumes.



Time evolution of fluid kinetic energy after switching-off the aerotaxis at time $t = 4$.

Stationary Plumes in the Presence of the Oxygen Cut-Off for Large Density Data

- Parameters $\beta = 10^2, \gamma = 10^4$ correspond to a 10-times higher reference cell-density
- Same deterministic initial data:

$$n_0(x, y) = \begin{cases} 1, & \text{if } y > 0.499 - 0.01 \sin((x - 1.5)\pi) \\ 0.5, & \text{otherwise} \end{cases}$$

$$c_0(x, y) \equiv 1, \quad \mathbf{u}_0(x, y) \equiv \mathbf{0}$$

We study the effects of the oxygen cut-off on the formation and stability of plumes by simply increasing the amount of cells.

